Review

Uveal melanoma modeling in mice and zebrafish

Quincy C.C. van den Bosch [a,b,d], Annelies de Klein [b,d], Robert M. Verdijk [c,d,e], Emine Kiliç [a,d,1], Erwin Brosens [b,d,1,*], on behalf of the Rotterdam Ocular Melanoma Study Group

[a] Department of Ophthalmology, Erasmus MC, Rotterdam, the Netherlands
[b] Department of Clinical Genetics, Erasmus MC, Rotterdam, The Netherlands
[c] Department of Pathology, Section of Ophthalmic Pathology, Erasmus MC, Rotterdam, The Netherlands
[d] Erasmus MC Cancer Institute, Rotterdam, The Netherlands
[e] Department of Pathology, Leiden University Medical Center, Leiden, The Netherlands

ARTICLE INFO

ABSTRACT

Despite extensive research and refined therapeutic options, the survival for metastasized uveal melanoma (UM) patients has not improved significantly. UM, a malignant tumor originating from melanocytes in the uveal tract, can be asymptomatic and small tumors may be detected only during routine ophthalmic exams; making early detection and treatment difficult. UM is the result of a number of characteristic somatic alterations which are associated with prognosis. Although UM morphology and biology have been extensively studied, there are significant gaps in our understanding of the early stages of UM tumor evolution and effective treatment to prevent metastatic disease remain elusive. A better understanding of the mechanisms that enable UM cells to thrive and successfully metastasize is crucial to improve treatment efficacy and survival rates. For more than forty years, animal models have been used to investigate the biology of UM. This has led to a number of essential mechanisms and pathways involved in UM aetiology. These models have also been used to evaluate the effectiveness of various drugs and treatment protocols. Here, we provide an overview of the molecular mechanisms and pharmacological studies using mouse and zebrafish UM models. Finally, we highlight promising therapeutics and discuss future considerations using UM models such as optimal inoculation sites, use of $BAP1^{mut}$-cell lines and the rise of zebrafish models.

1. Introduction

Uveal melanoma (UM) is the most common primary intraocular malignancy that arises after somatic changes in uveal melanocytes [1]. Clinical, histological, and genomic characteristics of primary UM are associated with clinical outcomes [2]. Up to 50% of patients will develop metastatic UM [3]. Even after successful treatment of the primary tumor, UM has a high probability of metastasizing to distant organs; partly due to the lack of noticeable lesions in the early metastatic stages of the disease [4,5]. Almost all UM patients have primary driver mutations in either Guanine nucleotide-binding protein Q (GNAQ), Guanine nucleotide-binding protein 11 (GNA11), Cysteinyl leukotreine receptor 2 (CYSLTR2) or Phospholipase C Beta 4 (PLCB4). These molecules act during G-Protein Coupled Receptor (GPCR) signalling in the MAPK/ERK pathway and YAP signalling [1]. These driver mutations can also be found in uveal nevi [6–8], which are considered as benign precursor

lesions of UM. Secondary driver mutations in Eukaryotic Translation Initiation Factor 1 A X-Linked (EIF1AX) [9], Splicing Factor 3b Subunit 1 (SF3B1) [10] or deubiquitinase BRCA1-associated protein-1 (BAP1) [11] are considered to delineate malignant transformation and are in general mutually exclusive, correlated to survival and associate with distinct transcriptomic profiles, methylation patterns and chromosomal aberrations [12,13]. BAP1, SF3B1 and EIF1AX all function in different molecular pathways: BAP1 is involved in activation of DNA damage repair system, regulation of ubiquitin signalling and assembly of the polycomb repressive complex [14], SF3B1 is essential in pre-mRNA splicing [15,16] and EIF1AX is one of the factors involved in remodeling the initiator complex during translation [17,18]. $EIF1AX^{mut}$ UM have a low risk to develop metastasis, $SF3B1^{mut}$-UM develop metastatic disease; but in general less rapidly compared to $BAP1^{mut}$-UM [19]. Patients with metastatic UM have a poor prognosis with a median overall survival of approximately 1 year [20,21]. The overall survival in metastatic

UM patients has been stable for the past decades [21], although some progress has been made in a subset of patients treated with immune-modulator Tebentafusp [22]. Transcriptome analysis elucidated the genetic composition of metastatic UM tends to resemble that of the primary tumor, although additional genetic alterations in the metastases can be present; indicating continuous oncogenic evolution after dissemination [23–25]. The immune-landscape of primary UM and metastases found in single-cell sequencing experiments indicated that cytotoxic T-cells predominantly express checkpoint marker Lymphocyte Activating 3 (*LAG3*) [26], implicating an important role for immune cells in the tumor microenvironment.

Clinical trials aimed at treating metastatic UM using a range of targeted strategies did not have the desired outcome [27], and thus the search for novel treatment modalities continues. For the past 40 years a popular method to discover and test drugs for a wide range of diseases is the use of animal models, especially mouse models [28]. Mouse tumor models have aided our understanding of anticancer drugs ranging from cytotoxic agents to biological therapeutics [29]. UM mouse models have been generated since 1980 by transplantation of human UM cells or *via* genetic engineering [30,31]. In an attempt to improve current models, several laboratories continue to illustrate successful engraftment of primary UM in immune-compromised mice [32–36]. To generate translatable models, the genetic background is of importance when designing a xenograft experiment. *BAP1*^{mut}/Monosomy 3 UM are present in the majority of patients that develop metastasis within a short period of 5 years after diagnosis [19]. Currently, there are many different UM cell lines with specific genetic profiles. A few *BAP1*^{mut} cell lines have been established (Supplementary table 1), but generally these tumor derived cell lines proliferate poorly *in vitro* [37]. There are 3 known cell lines derived from *SF3B1*^{mut} UM and 2 known cell lines derived from *EIF1AX*^{mut} UM (Supplementary table 1). Remarkably, these latter *EIF1AX*^{mut} cell lines are atypical and may not fully represent *EIF1AX*^{mut} UM as both have been established from metastasizing *EIF1AX*^{mut} UM [37,38]. Only a few cell lines are characterized in full detail with known driver mutations, secondary mutations and copy number variations (Supplementary table 1). The use of UM derived cell lines has the advantage that these cell lines often display the corresponding copy-number variations [39], but long term cultivation of UM cells reduces gene expression compared to primary tumors [40]. Next to mouse models, the use of zebrafish (*Danio rerio*) models has recently been gaining popularity to study UM [41].

Here, we describe a comprehensive overview of the current literature of all mouse and zebrafish models generated with uveal melanoma cell lines or *via* transgenesis. We provide an overview of all compounds tested in xenograft models and their anticancer-effect, illustrate drawbacks of the current models and provide suggestions for future improvements.

2. Structured literature search: Uveal melanoma animal models

We searched for peer-reviewed studies between 01 and 01–1946 and 11-07-2023 in 4 databases: Embase, Medline ALL, Web of Science Core Collection and Google Scholar (For details see Supplementary methods). In brief, each database search was designed to find *in vivo* ocular UM models using either mice or zebrafish which generated a list of 1570 publications. Inclusion criteria for this review were: 1) xenografts using a human uveal melanoma cell lines in mice or zebrafish and 2) transgenic mouse or zebrafish models that develop ocular melanoma. UM animal models that use cell lines harbouring B-Raf Proto-Oncogene, Serine/Threonine Kinase (*BRAF*) / NRAS Proto-Oncogene, GTPase (*NRAS*)-mutated melanoma cells [42] (*n* = 83) were excluded. Additionally, models developed with the highly aggressive mouse cutaneous melanoma line B16 or Greene's hamster-melanoma cell line [43] (*n* = 66) were also excluded in this survey. (Fig. 1A, Supplementary fig. 1). Molecular status of cell lines discussed in xenograft models are shown in Supplementary table 1. For the purpose of this review, we excluded

studies using other animals than zebrafish or mice (*e.g.* cats, rats and rabbits) due to the large amount of literature available on these two models.

3. Xenograft uveal melanoma models

Xenograft models included in this review have been used to elucidate molecular signalling in specific pathways, modulation using specific pharmaceutical targets aimed at UM specific and generic pathways or using antibody-based/oncolytic virotherapies. Full-text assessment of 288 eligible studies revealed 139 studies using Gαq/11^{mut} or UM cells without known driver mutations (Fig. 1A, Supplementary Fig. 1). From the selected Gαq/11$^{mut/WT}$ studies, a total of 188 mouse models were generated, mostly using subcutaneous inoculations (Fig. 1C), and a total of 13 zebrafish xenografts (*section 3.5*). The cell line that has been used most often is 92.1 (Fig. 1C). An overview of the cell lines used, aim of the study and inoculation site per murine study is described in supplementary table 2. In this section, we summarize and discuss uveal melanoma xenograft models generated by inoculation of Gαq-mutated melanocytes or human uveal melanoma cell lines.

3.1. Generating xenograft models in mice

Xenograft models are generated by inoculation of human tumor cells in mice. This method is a relatively straightforward tumor model, in which human tumor cells are traditionally inoculated subcutaneously [29]. However, subcutaneous inoculation does not reflect the complexity of the original tumor and its environment [29], and inoculation can be improved by injecting cells at the place of anatomical origin (*e.g.* ocular injection for primary UM cells or hepatic injection for metastatic UM cells; Fig. 1D). Xenograft models for UM have come a long way since the first successful transplant in 1980. In this model, a human choroidal melanoma was transplanted into the posterior segment in the eye of a nude mouse and illustrated successful engraftment [44]. Our literature search indicates that the majority of UM xenografts were developed using subcutaneous inoculation of UM cells (Fig. 1B, Supplementary table 2). To study UM in the most prevalent metastatic loci, direct hepatic inoculation has been performed in 9 studies (Fig. 1B, Supplementary table 2). Thirteen studies describe the use of intrasplenic inoculation (Fig. 1B, Supplementary table 2), to replicate haematogenous dissemination and subsequent liver metastasis [45]. Intravenous inoculation to simulate disseminated cells in the circulation results in micro metastasis after 6 weeks, but fail to grow into large metastasis [46]. To simulate the microenvironment of the primary tumor, a total of 30 xenograft models have been generated by intra-ocular inoculation (Fig. 1B, Supplementary table 2). Liver metastasis after ocular inoculation is dependent of the cell line: 92.1, Mel290, MP41, OMM1 and OMM2.3 are able to develop liver metastasis [33,47–51], whereas UMT2 and UMT42 failed [32]. Due to the nature of working with tumor cells derived from patients, these models are not suitable to investigate tumor initiation (which requires genetically engineered models) and are typically used as models to study tumor growth and progression.

3.2. Studying UM tumor growth and metastasis in murine xenograft models

In general, UM-tumors harbour one of the four mutually exclusive primary driver mutations: in over 90% of the UM patients either in the Guanine nucleotide-binding protein Q (*GNAQ*) [52] or the Guanine nucleotide-binding protein 11 (*GNA11*) [53] (both referred here as Gαq/11). In approximately 5% of UM, driver mutations in Cysteinyl leukotreine receptor 2 (*CYSLTR2*) [54] or Phospholipase C Beta 4 (*PLCB4*) [55] are present [1]. Both genes participate in G-Protein-Coupled Receptor (GPCR) signalling *via* similar pathways. The two primary signalling pathways involved are the mitogen-activated protein kinase kinase (*MEK*) / extracellular signal-regulated kinase (*ERK*)
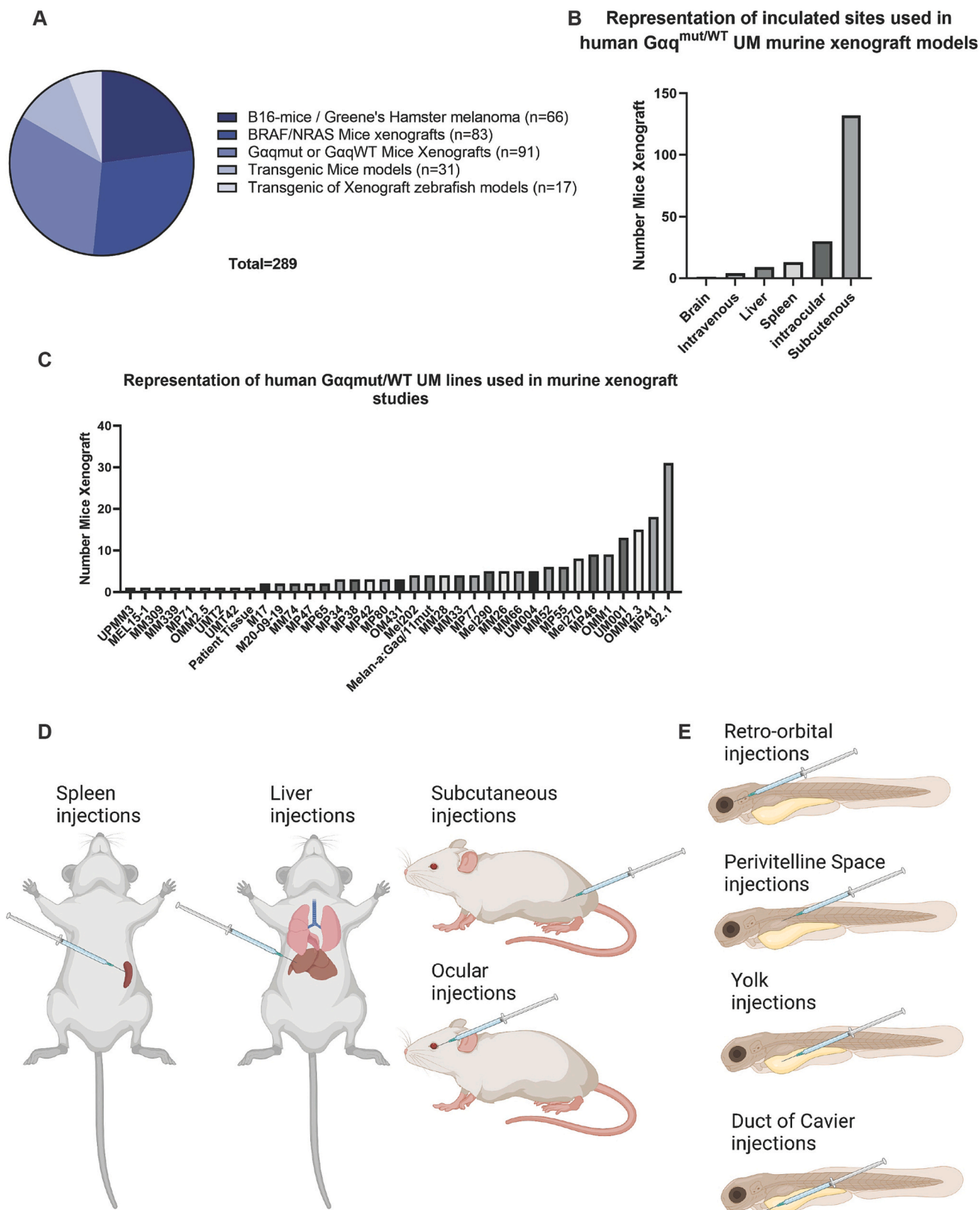
Fig. 1. Representation of xenografts models used in the selected studies. A) Overall distribution of selected studies. B) Overview of inoculation sites of Gαq^{mut}-based xenografts from 91 studies: Brain $n = 1$, Intravenous $n = 4$, Hepatic $n = 9$, Spleen $n = 13$, Intraocular $n = 30$, Subcutaneous $n = 132$. C) Overview of used cell lines in Gαq^{mut}-based xenografts. Known BAP1-negative cell lines are MP38, MP46, MP65, MM28. D and E) Schematic representation of inoculation sites used in xenografts described in review in mice and zebrafish larvae.

pathway and the Yes1 Associated Transcriptional Regulator (*YAP*) signalling pathway [1]. CYSTLR2 and Gαq/11 activate YAP signal transduction to activate genes involved in cell proliferation [56]. Additionally, CYSLTR2, Gαq/11 and PLCB4 activate MEK/ERK signalling *via* Phosphatidylinositol 4,5-bisphosphate(PIP$_2$) and protein kinase C (PKC); inducing cell proliferation [57]. *GNAQ* mutations are not predictive of patient outcome [58], and despite the association of *GNA11* with prognosis relevant genetic alterations [59], both mutations are also found in non-aggressive blue nevi [53]. Targeting Gαq/11-signalling could provide a therapy for the majority of patients with UM due to the high prevalence of *GNAQ* or *GNA11* mutations. Understanding how Gαq/11-signalling is affected by *Gαq/11$^{Q209P/L}$* mutations is pivotal to develop targeted treatments. Xenograft models have aided in identifying multiple signalling nodes and their corresponding mechanisms. Genetically modified mouse models illustrated that Gαq/11 proteins are folded by Resistance to inhibitors of cholinesterase-8 A (*RIC-8 A*), a chaperone regulating most Guanine nucleotide binding alpha proteins [60]. Mice that are deficient for Ric-8a harbored a lower UM tumor burden compared to wild-type mice after inoculation of murine Gαq/11^{mut}-melanocytes, illustrating an important role of RIC-8 A in Gαq/11^{mut} expression [61]. One of the pathways regulated by GPCRs is the Hippo-YAP pathway, which can either activate or repress nuclear YAP depending on the GPCR [62]. YAP is canonically activated *via* the Hippo-signalling pathway which regulates cell proliferation, stemness and reacts to environmental cues [63]. Unlike *BRAF^{mut}* melanoma cells, Gαq/11^{mut} melanoma cells demonstrate nuclear expression of YAP [64]. Inhibition of YAP by verteporfin in 92.1-xenografts

elucidated that YAP is essential for UM growth *in vivo*. This is further supported as YAP inhibitor MGH-CP1 also reduced tumor burden in 92.1-xenografts [65]. In UM, nuclear YAP expression is regulated by Rho-family guanosine triphosphatases (Rho-GTPase) [66]. Rho-GTPases are involved in many processes such as cell adhesion, endocytosis, migration and cell cycle regulation [67]. Rho-GTPase is activated *via* ADP-ribosylation factor 6 (ARF6) signal transduction. Gαq/11^{mut} recruits ARF6, which subsequently acts as a complex to activate Rho-GTPase (Fig. 2). Inhibition of ARF6 using short hairpin-RNA or NAV-2729 in Mel202-xenografts revealed ARF6 to be crucial for UM growth *in vivo* [68]. The overall Gαq/11^{mut}-signalling pathway driving UM proliferation are illustrated in Fig. 2.

A major advantage of xenograft models is the ability to study putative metastatic modulators found in UM. One of the first metastatic factors studied in metastatic UM models was NME/NM23 Nucleoside Diphosphate Kinase 1 (*NM23-H1*). *NM23-H1* is the first described metastasis suppressor [69]. Lack of NM23-H1 protein expression correlates with UM prognosis [70] and *in vivo* models using *NM23-H1^{high}* cells (92.1) had an increased metastatic burden compared to *NM23-H1^{low}* cells (OM431) [71]. *NM23-H1* is known to respond to reactive oxygen species [72], therefore the link between hypoxia/angiogenesis and *NM23-H1* could be of interest to study in context of high-risk UM. An important regulatory mechanism for metastatic processes in high-risk UM is liver secreted hepatocyte growth factor (HGF) and its receptor MET proto-oncogene, receptor tyrosine kinase (c-MET) [73,74]. c-MET expression is present in primary UM and elevated in metastatic UM [75]. Furthermore, c-MET can be cleaved into a soluble form [76]
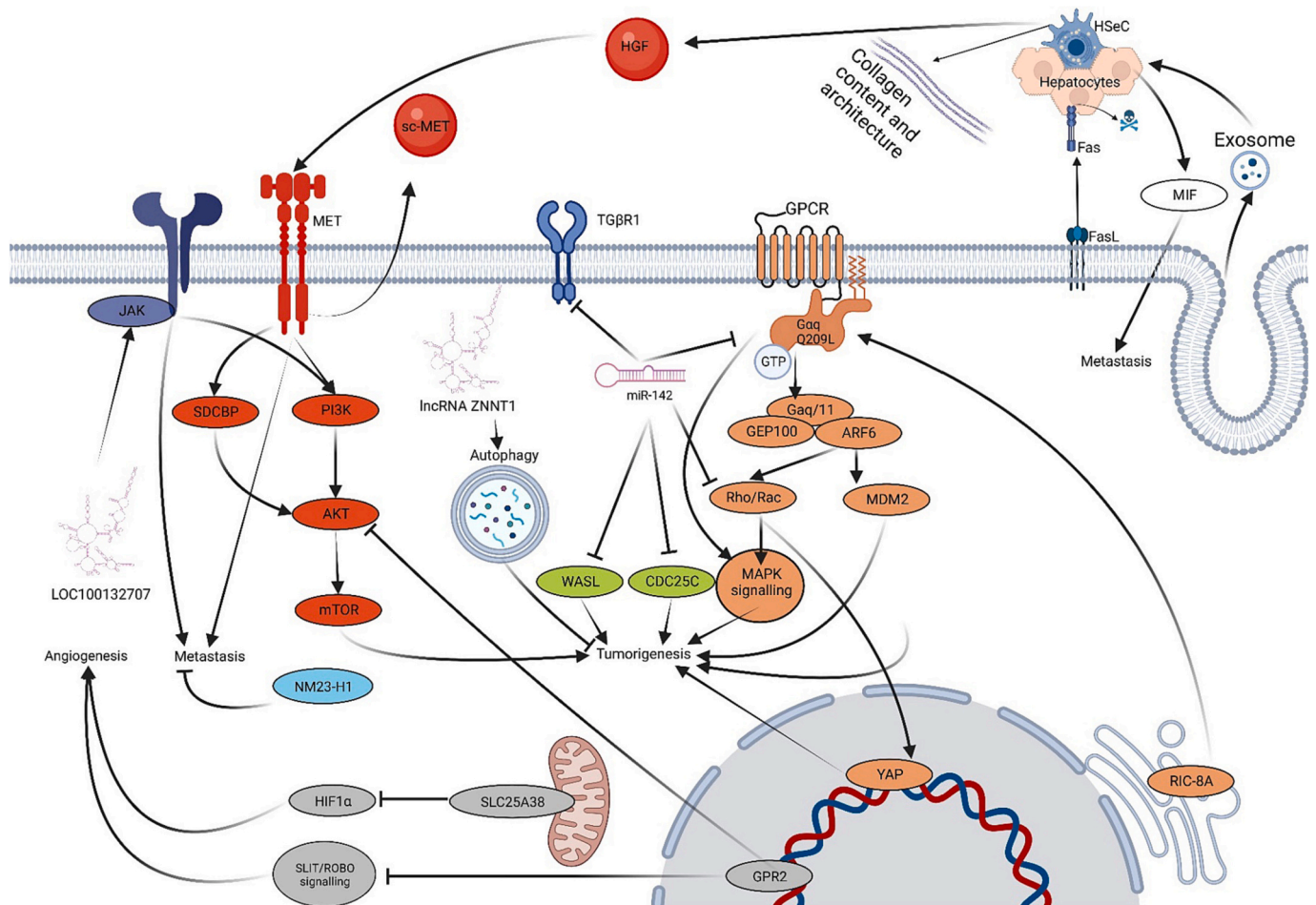
Fig. 2. Schematic overview of identified biomarkers using xenograft mouse models. In blue: JAK-activation, Red: AKT-mTOR-signalling, Orange: Gnαq/11-signalling, Gray: genes involved in angiogenesis, Green: genes involved in tumor growth regulated by miRNA. Sharp arrows indicate stimulation, blunt arrows indicate inhibition. (For interpretation of the references to colour in this figure legend, the reader is referred to the web version of this article.)

(Fig. 2), which is increased in serum upon metastatic disease [77]. The HGF/MET pathway activates multiple pro-tumorigenic signalling nodes in UM, such as MEK/ERK signalling and PI3K/AKT/mTOR signalling, which both are capable to induce cell proliferation, survival and migration [78]. HGF is secreted by hepatic stellate cells (HSteCs) [79] that interact with sinusoidal endothelial and hepatic epithelial cells [80]. Metastatic mouse models (using splenic inoculation) illustrated that HSteCs are able to alter collagen architecture which increased metastatic loci and sizes [81]. Stimulation of HSteCs to secrete pro-metastatic factors can be induced *via* exosomes that are released by UM cells. Pre-treating mice with exosome from 92.1-cells increased metastatic burden due to elevated levels of macrophage migration inhibitory factor (MIF) compared to non-treated mice (Fig. 2) [82]. Once metastases are seen in the liver, treatment options are limited, resulting in poor prognosis [83]. The poor prognosis is in part due to the ability of metastatic UM cells to induce cell death of healthy hepatocytes [47] (Fig. 2, FasL-pathway). Based on the current models, UM metastasis seems to rely on the HGF/MET-signalling pathway, which is stimulated by the organ-specific environment of the liver. The HGF/MET mechanism is independent of secondary driver mutations shown by *in vivo* experiments utilizing cell lines originating from *SF3B1^{WT}/BAP1^{WT}* tumors (92.1, Mel270, OMM1). However, due to the high risk of metastasis of *BAP1^{mut}*-UM, several groups decoded genetic material of UM to identify novel genes. Characteristic chromosomal aberrations such as chromosome 3 loss (partial or fully) and gain of chromosome 8q in primary UM is a strong predictor of high-risk UM [84]. Gene expression analysis focusing in on these chromosomal aberrations identified Solute Carrier Family 25 Member 38 (*SLC25A38*) [85] and Syndecan Binding Protein (*SDCBP*) [86] as potential factors involved in high-risk UM. Both factors increased metastatic burden in xenograft models, where lack *SLC25A38* induced angiogenesis [85] and elevated levels of SDCBP increased invasion *via* the HGF/MET mechanism [86].

Next to coding RNA, the role of non-coding RNA (ncRNA) in UM is starting to unfold. Non-coding RNAs are able to promote tumorigenesis and metastasis *via* key contribution in many molecular pathways [87,88]. Non-coding RNA in UM has been investigated predominantly *in vitro* [87], however there are few xenograft models illustrating the role of three different ncRNAs *in vivo*. Long non-coding RNA ZNF706 Neighbouring Transcript 1 (*ZNNT1*) was investigated *in vitro* where it functions as an autophagy activator in UM cell lines. Overexpression of *ZNNT1* inhibited tumor growth *in vivo*, suggesting stimulation of autophagy could provide anticancer properties in UM [89]. Another long non-coding RNA studied is PAXIP1 Antisense RNA 2 (*PAXIP1-AS2*), after it was identified to be upregulated in metastatic UM [90]. *PAXIP1-AS2* expression was correlated to JAK/STAT signalling which is known to induce invasion *via* the Signal Transducer and Activator of Transcription 3 (STAT3)-twist family bHLH transcription factor 1 (TWIST1) axis [91]. *In vivo* downregulation of *PAXIP1-AS2* inhibited tumor growth due to downregulation of JAK2, MMP9 and MMP2 in MM28-xenografts [90]. The last model studying ncRNA illustrated the role of microRNA in UM development. MicroRNA142 expression was downregulated in UM cell lines compared to healthy uveal melanocytes and was shown to inhibit multiple generic proliferation genes, but most interestingly also targets *GNAQ* (Fig. 2). Upregulation of microRNA142 *in vivo* significantly reduced tumor growth compared to non-treated xenografts; pinpointing microRNA142 as a potential tumor suppressor in UM [92].

3.3. Pharmacological studies in murine UM xenograft models

The primary advantage of *in vivo* models is the capacity to investigate efficacy of drugs within a complex environment. Xenograft models commonly use severe compromised immune deficient (SCID) mice facilitating the engraftment of human uveal melanoma (UM) cells. Therefore, it is important to acknowledge that the translational relevance of these models to clinical practice may be limited [29]. Here, we present an overview of pharmacological investigations conducted in

xenograft mice using human UM cell lines. Our search and filtering process identified 56 publications, comprising 21 studies examining combination treatments and 35 studies examining stand-alone treatments. Each compound, combinations and cell lines used per study is summarized in Tables 1–3, Supplementary table 3 and are illustrated in Fig. 3.

3.3.1. MEK-ERK pathway

As described above, GαqQ209P/L mutations are known to activate the MEK-ERK pathway [1,56]. MEK-ERK signalling activation is frequently identified in many other cancer types [93], which led to the development of several MEK inhibitors (MEKi). Although MEK inhibition is used in clinical practice for cutaneous melanoma [94], UM patients are non-responsive [95]. MEKi resistance in UM patients is in part due to fibroblast/hepatocyte secreted HGF and/or Neuregulin 1 (NGR1). These secreted molecules are able to activate PI3K-AKT signalling *via* MET and EBBR2/3, which promoted tumor growth in UM001-xenografts. This suggests a mechanism that could explain tumor growth despite MEK inhibition in UM patients [96]. However, trametinib (MEKi) is able to inhibit tumor growth and metastasis formation in UM001/UM004-xenograft models [45]. The discrepancy between MEKi resistance in humans and mice is explained due to the incompatibility of murine Hgf with human MET receptors; which thus lack alternative tumor promotion *via* MET-PI3K-AKT signalling in xenograft-models [97].

To overcome MEKi resistance due to activated alternative pathways, many studies investigated pharmacological responses after targeting multiple targets simultaneously (Table 1). By targeting multiple proteins within the MEK-ERK pathway, such as FAK or PKC (Fig. 2), one could enhance downstream inhibitory effects. Inhibition of MEK together with Focal adhesion kinase (FAK) [56,98] or PKC [99] in various xenograft models (Mel270, OMM2.3, 92.1 and murine-melanocytes expressing human *GNAQ^{Q209L}*) indeed improved therapeutic outcomes. In a similar fashion, inhibition of Rho-GTPases using Cerivastatin synergyzed with MEKi in UPMM3-xenografts (*BAP1^{mut}*) and demonstrated strong tumor volume reduction. Protein analysis revealed Cerivastatin inhibits p-AKT and YAP; yet when combined with Trametinib a stronger inhibition was seen with additional upregulation of caspase-3 and PARP1 [100]. Ohers have instead inhibited the MEK-ERK pathway in combination with proteins involved in other pathways. Inhibiting the MET-PI3K-AKT pathway *via* MET, PI3K, AKT or its downstream node mTOR in combination with inhibiting the MEK-ERK pathway were shown to act synergistically *in vitro* [101]. Several *in vivo* studies support these finding by illustrating reduce tumor growth *in vivo* [102,103], while some studies additionally demonstrated its potential to inhibit macrometastasis in 92.1 xenografts [104,105]. Interestingly, inhibition of PKC and PI3K is only effective in Gαq-mutant cells (92.1) and not for Gαq/11WT UM cells (OMM1) [106]. This could suggest that driver mutations are crucial to develop effective personalized therapies.

Another important aspect in UM progression is the DNA methylation status of UM, as it is know that the methylation profile differs per subtype [107]. An important class of proteins responsible for DNA methylation are DNA methylation transferases (DNMT). By adding methylgroups onto the DNA which silences gene expression, these proteins play a crucial role in gene regulation [108]. For instance, inhibition of DOT 1 like histone lysine methyltransferase (DOT1L) inhibited tumor growth *in vivo* by abrogating NAD+ synthesis [109] and combined inhibition of DNMTs and MEK in 92.1- and Mel270-xenografts reduced tumor volume due to upregulation of pro-apoptotic protein BIM [110]. Resisting cell-death is an hallmark of cancer [111], making upregulating pro-apoptotic proteins an interesting mechanism for treating cancer. Inducing apoptosis and thus reducing tumor volume can be achieved *via* multiple signalling nodes, such as *via* MDM2 proto-oncogene (MDM2). MDM2 is a negative regulator of p53, which is well known for its tumor suppressor function. MDM2 induces p53 degradation, as such inhibiting MDM2 prevents p53 degradation and allows p53 to act as a tumor suppressor by inducing apoptosis [112]. Inhibition of the MEK-ERK

Table 1

Overview of compounds studied in UM xenograft models targeting the MEK-ERK pathway Compounds are used as a single dose, or in combination with other molecules targeting other pathways. For each study the used cell line used to generate xenografts are shown with the corresponding compound effect after treatment. In bold BAP1neg UM cells are highlighted. Abbreviations: mitogen-activated protein kinase kinase (MEK1/2), Focal adhesion kinase (FAK), protein kinase C (PKC), MDM2 proto-oncogene (MDM2), Cyclin dependent kinase 4 (CDK4), Cyclin Dependent Kinase 6 (CDK6), mammalian target of rapamycin (mTOR), Phosphoinositide 3-kinases (PI3K), Deoxyribonucleic acid (DNA), P62, Poly(ADP-ribose) polymerase (PARP), Ataxia Telangiectasia Mutated (ATM), Ataxia Telangiectasia And Rad3-Related Protein (ATR), reactive oxygen species (ROS). * cells were pretreated with 10uM SGC0946 for 10 days pre-inoculaton.

Drug	Target	Dosage (mg/kg)	Administration	Therapy	Cell line	Compound effect	Ref.
Trametinib	MEK1/2	1	Daily	single	UM001, UM004	Reduction in tumor volume, inhibits macrometastasis	[45]
VS-4718	FAK	10	Twice daily	single	OMM2.3, Mel270	Reduction in tumor volume	[98]
VS-4718	FAK	50	Twice daily	Dual	92.1, OMM2.3	Reduction in tumor volume	[56]
Trametinib	MEK1/2	1	Daily				
Sotrastaurin	PKC	20, 40, 80	Daily	Dual	Melan-a melanocytes expressing GNAQ^{Q209L}, 92.1	Reduction in tumor volume	[99]
Binimetinib	MEK1/2	3,5	Twice daily				
CGM097	MDM2	100	5 times per week				
Ribociclib	CDK4, CDK6	75	5 times per week				
Binimetinib	MEK1/2	3.5	5 times per week	Dual	MP42, **MP46**, MM33, MM52, MM66	Reduction in tumor volume	[103]
Sotrastaurin	PKC	120	5 times per week				
Everolimus	mTOR	5	5 times per week				
Pictilisib	PI3K	100	5 times per week				
Decitabine	DNMT	1	3 times per week	Dual	92.1, Mel270	Reduction in tumor volume	[110]
Trametinib	MEK1/2	0.5	Daily				
Chloroquine	P62	40	Daily				
Temozolomide	DNA	100	Daily	Dual	OMM2.5	Reduction in tumor volume	[117]
Trametinib	MEK1/2	1	Daily				
Chloroquine	P62	50	Daily	Dual	92.1	Reduction in tumor volume	[118]
Dacarbazine	DNA	50	3 times per week				
Dacarbazine	DNA	40	1–5 times per 4 weeks				
Olaparib	PARP	50 or 100	5 times per week				
Sotrastaurin	PKC	240	5 times per week				
CGM097	MDM2	100	5 times per week	Dual	MP41, **MP55**, MP77, MM33, MM52, MM66	Reduction in tumor volume	[119]
AZD0156	ATM	2.5 or 5	3 times per week				
Ceralasertib	ATR	12.5	3 times per week				
Everolimus	mTOR	5	5 times per week				
Fotemustine	DNA	20	Day 1 and Day 22				
Elesclomol	ROS	25 or 50	5 times per week	Dual	92.1	Reduction in tumor volume	[115]
Binimetinib	MEK1/2	3	Daily				
withaferin A	MET and MEK1/2	8 or 12	Daily	single	92.1	Reduction in tumor volume, some mice CR	[104]
Sorafenib	RAS/RAF	60	Daily	Dual	92.1	Reduction in tumor volume, inhibit macrometastasis	[105]
Lenalidomide	AKT	100	Daily				
selumetinib	MEK1/2	25	Not specified	Dual	92.1	Reduction in tumor volume	[102]
MK2206	AKT	150	Not specified				
Sotrastaurin	PKC	80	5 times per week	Dual	92.1, OMM1	Reduction in tumor volume	[106]
BYL719	PI3K	50	5 times per week				
SGC0946	DOT1L	-*	None*		OMM2.3	Reduction in tumor volume	[109]
Trametinib	MEK	1	3 times per week	Dual	UPMM3	Reduction in tumor volume	[100]
Cerivastatin	Rho	2	3 times per week				

pathway and MDM2 reduced tumor volume in multiple xenograft models. In comparison to MEK-ERK and PI3K-AKT pathway inhibition, tumors were smaller after inhibition of MEK-ERK pathway and MDM2 [103].

Another way to induce apoptosis is *via* reactive oxygen species (ROS), where an influx of ROS acts as a signal to activate apoptosis [113]. The compound elesclomol has the ability to transport copper to mitochondria, which in turn generates a large amount of ROS [114]. Elesclomol was sensitive to Gαq/11^{mut} cells (92.1, OMM1, OMM2.3) whereas Gαq/11^{WT} cells (Mel290) were resistant. In 92.1-xenografts elesclomol inhibited tumor growth, but more interestingly when combined with MEKi tumors size shrank to nearly 50% smaller than at the start of treatment [115]. The fact that Gαq/11^{WT} cells were resistant to the influx of ROS, suggests Gαq/11^{mut} cells are more vulnerable to ROS while at the same time illustrate Gαq/11^{WT} cells utilize different mechanisms to survive and thrive.

MEKi have also been combined with autophagy inhibitors in UM xenografts. Autophagy plays a key role in degradation of cellular material while also providing precursor molecules and energy for cellular processes [116]. In cancer, autophagy plays a complicated role and it is often unclear whether the best strategy is inhibition or stimulation to achieve cellular apoptosis [116]. Inhibition of autophagy using chloroquine has been studied in clinical trials, where *BRAF, KRAS and EGFRvIII* mutations are markers of tumor progression that depend on active autophagy [116]. In UM, autophagy inhibition using chloroquine was combined with MEKi. This reduced tumor growth in OMM2.5-xenografts [117] and 92.1-xenografts due to downstream inhibition of pro-autophagy protein P62 [118]. However, autophagy dependence is likely to differ between UM subgroups as an OM431-xenograft model showed tumor regression upon autophagy stimulation [89]. When used in isolation, MEKi seems inadequate in halting tumor progression. Nevertheless, when combined with other compounds, a synergistic effect is observed. Using combined inhibition of MEK-ERK and PI3K-AKT pathways, some models demonstrated inhibition of macro-metastasis and in some cases even resulted in complete remission. Additionally, primary driver mutations are important to take into account before deciding on treatment options. Inhibition of PKC or PI3K failed to inhibit tumor progression in Gαq/11^{WT} cells, as did ROS induction *via* elesclomol; whereas these strategies were more effective in Gαq/11^{mut} cells.

Table 2

Overview of compounds studied in UM xenograft models targeting the AKT-PI3K-mTOR pathway alone or in combination with other pathways. For each study the used cell line used to generate xenografts are shown with the corresponding compound effect after treatment. In bold BAP1neg UM cells are highlighted. Abbreviations: MET proto-oncogene, receptor tyrosine kinase (MET), Phosphoinositide 3-kinases (PI3K), mammalian target of rapamycin (mTOR), mitogen-activated protein kinase kinase (MEK1/2), Rat sarcoma / rapidly accelerated fibrosarcoma (RAS/RAF), AKT serine/threonine kinase (AKT), protein kinase C (PKC).

Drug	Target	Dosage (mg/kg)	Administration	Therapy	Cell line	Compound effect	Ref.
Crizotinib	MET	50, 75, 100	5 times per week	single	92.1, OMM2.3	No reduction in tumor volume, inhibits macrometastasis	[124]
4-O-(4′-o-alpha-D-Glucopyranosyl)-caffeoyl quinic acid	PI3K	5 or 10	5 times per week	single	**MP65**	Reduction in tumor volume	[134]
AZD8055	mTOR	200 BSA; 5 AZD	1 time per week	single	Mel202	Reduction in tumor volume	[121]
ICG-001	mTOR	50	5 times per week	single	Mel270	Reduction in tumor volume	[122]
Everolimus	mTOR	2	3 times per week	single	MP34, MP41, **MP46, MP55**	Reduction in tumor volume	[37]
Everolimus	mTOR	2	5 times per week	Dual	MM52, MM66	Reduction in tumor volume	[123]
Pictilisib	PI3K	100	Daily				
withaferin A	MET and MEK1/2	8 or 12	Daily	single	92.1	Reduction in tumor volume, some mice CR	[104]
Sorafenib	RAS/RAF	60	Daily	Dual	92.1	Reduction in tumor volume, inhibit macrometastasis	[105]
Lenalidomide	AKT	100	Daily				
Cordycepin	Hsp90	2–20	3–4 times per week	Dual	92.1, **MP46**	Reduction in tumor volume	[125]

Table 3

Overview of compounds studied in UM xenograft models targeting G-protein coupled Receptor signalling alone or in combination with other pathways. For each study the used cell line used to generate xenografts are shown with the corresponding compound effect after treatment. In bold BAP1^{mut} cell lines are highlighted. Abbreviations: C-X-C motif chemokine receptor 1/2 (CXCR1/2), C-X-C motif chemokine receptor 4 (CXCR4), melanocortin 1 receptor (MC1R), Guanine nucleotide-binding protein Q or Guanine nucleotide-binding protein 11 (Gαq/11, Gαq/11^{mut}).

Drug	Target	Dosage (mg/kg)	Administration	Therapy	Cell line	Compound effect	Ref.
Ladarixin	CXCR1/2	15	Daily	single	UM001, UM004	Reduction in tumor volume	[133]
CXCR4-antagonist 4	CXCR4	0.3	Daily	single	OMM2.3	Inhibit macrometastasis	[134]
CXCR4-antagonist 26	CXCR4	10	Daily	single			
MSX-122	CXCR4	10	Daily	single	OMM2.3	inhibit macrometastasis	[50]
225Ac-DOTA-MC1RL	MC1R	59.2 kBq	Not specified	single	Mel270	Reduction in tumor volume, inhibit macrometastasis	[137]
FR900359	Gαq/11	0.1, 0.3, 1.0, 3.0	3–5 days	single	MP41, **MP46**	Reduction in tumor volume	[138]
FR900359	Gαq/11	0.3 or 0.6	3–4 days	single	**MP46**	Reduction in tumor volume	[140]
N157	IRS1/2	50	3 days per week	single	92.1, **MM28**	Reduction in tumor volume	[142]
YM-254890	Gαq/11	0.3–0.4	Daily	Dual	UM001	Reduction in tumor volume	[143]
Linsitinib	IGF1R	25–40	Daily				
GQ127	Gαq/11^{mut}	10 or 30	Daily	single	MP41	Reduction in tumor volume	[139]
GQ262	Gαq/11^{mut}	5, 15, 30	Daily	single	MP41	Reduction in tumor volume, some mice CR	[145]

3.3.2. PI3K-AKT-mTOR pathway

The PI3K-AKT-mTOR pathway in UM is linked to both tumorigenesis, metastatic capacity and MEKi resistance [78]. The major upstream activator MET and its ligand HGF to initiate the cascade by activating PI3K, AKT and eventually mTOR to drive cell proliferation and migration [73,74]. Several drugs targeting PI3K [120] or mTOR [37,121,122] were studied as single compound agents; all showing capacity to inhibit tumor growth in MP65-, Mel202-, Mel270-, MP34-, MP41-, MP46- and MP55-xenografts. Inhibiting two nodes in the PI3K-AKT-mTOR pathway (PI3K and mTOR) simultaneously improved efficacy compared to single agent treatments in xenografts with metastatic cell lines (MM52, MM62) [123]. Interestingly, inhibition of MET did not alter tumor growth *in vivo*; however, it did prevent the formation of macrometastasis in OMM2.3- and 92.1-xenografts [124]. MET inhibition did not alter expression levels of PI3K, AKT or mTOR, which suggests MET-signalling is involved in metastasis but uses an alternative pathway. Simultaneous inhibition of MET and RAF/RAS by Withaferin A did show improved tumor growth inhibition in 92.1-xenografts. But most interestingly, 29% of mice showed complete remission after treatment with Withaferin A [104]. Recently, a novel way to inhibit UM growth investigated nucleotide-synthesis pathways and the anticancer ability of non-typical nucleotide structures, such as 3′-deoxyadenosine; also known as cordycepin. Inhibition of adenosine deaminase combined with adding cordycepin in UM cells induced a dose-dependent response *in vitro*.

Mechanistically, this treatment inhibited Heatshock protein 90 (Hsp90) which in turn lead to degradation of HIF1a, AKT, ERK and EGFR. *In vivo* inhibition of adenosine deaminase or Hsp90 were evenly effective; but combination treatment showed a strong synergistic effect by reducing the tumor burden significantly compared to single treatments [125].

3.3.3. G-protein-coupled Receptors: CXCRs, MC1R, Gαq/11 pathways

GPCRs are membrane receptors with an wide array of functions. GPCR-signalling is orchestrated *via* G alpha, beta and gamma proteins, where conversion of GDP to GTP leads to signalling activation [126]. Most driver mutations in UM are identified in *GNAQ* and *GNA11* [1], which both are G alpha proteins. Inhibition of either GPCRs or GNAQ/GNA11 themselves could provide targeted treatment for a large number of UM patients. C-X-C motif chemokine receptor 4 (CXCR4) was identified in high-risk UM [127,128] as a potential GPCR involved in directional migration of UM towards the liver [129]. However, this mechanism is not supported by all experts in the field as others have reported that CXCR4 is not of clinical relevance but C—C motif chemokine receptor 7 (CCR7) is [130]. Despite the discordance, this molecule has been employed in the creation of MRI-based contrast agents for the detection of UM micrometastasis [131,132]. So far, a range of GPCRs (CXCR1, CXCR2, CXCR4, melanocortin 1 receptor (MC1R) and Gαq^{mut} proteins) has been targeted *in vivo* with several compounds. Inhibiting CXCR1 and CXCR2 reduced Ki-67,
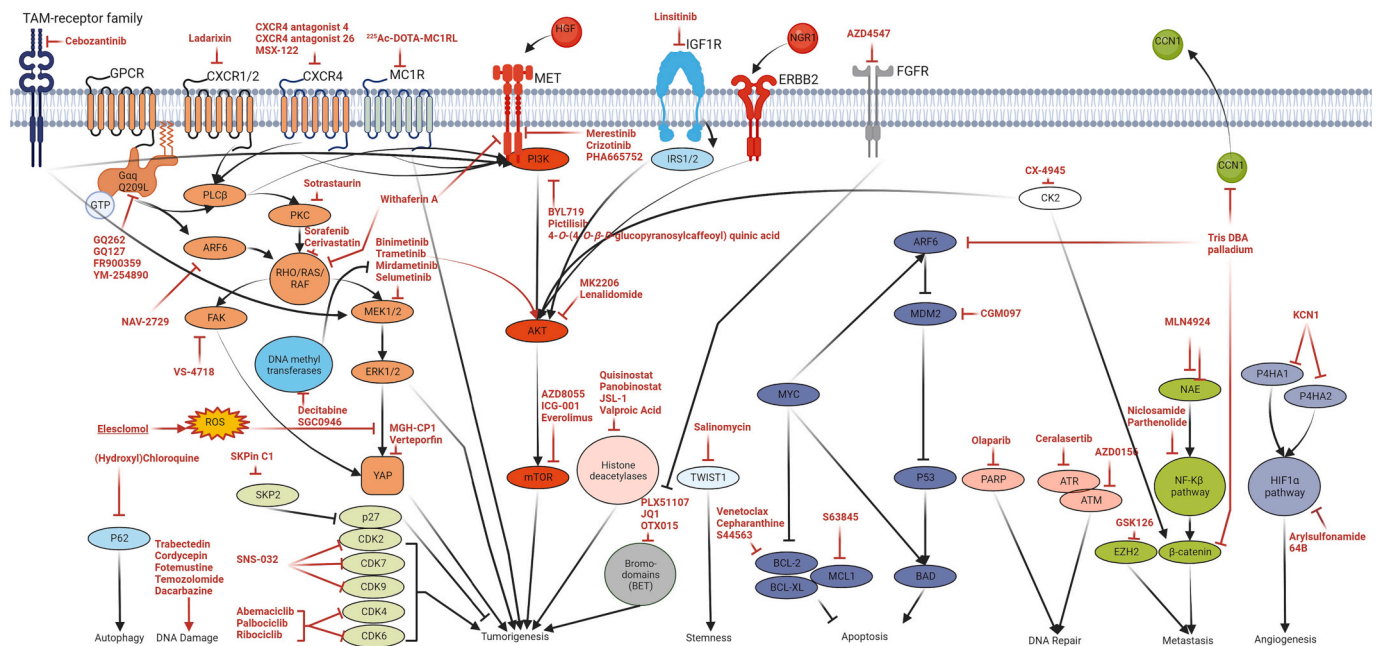
Fig. 3. Schematic overview of evaluated compounds in xenograft UM mouse models. Text in red represents the compounds evaluated in xenograft models with their targets. Pathways driving tumorigenesis in UM that have been inhibited with compounds are the Gaq/11-MEK1/2-ERK-pathway (Orange), PI3K-AKT-mTOR-pathway (Red), Apoptosis pathways (Light blue), DNA repair (pink), Angiogenesis (Light purple), NF-κB-pathway (Green), Cyclin-dependent kinases (light Green), autophagy, (Light Yellow) Bromodomains, (light Red) histone deacetylases and (white) stemness factor TWIST1. Sharp arrows indicate stimulation, blunt arrows indicate inhibition. (For interpretation of the references to colour in this figure legend, the reader is referred to the web version of this article.)

phosphorylated-*Nuclear factor kappa-light-chain-enhancer of activated B cells* (NF-κB) and pAKT levels which slowed down tumor growth in UM001- and UM004-xenografts [133], whereas inhibition of CXCR4 was able to reduce hepatic metastatic burden in metastatic xenograft models (OMM2.3) [50,134].

Instead of using UM-specific GPCRs, a more general approach is to target MC1R; a GPCR involved in induction of pigmentation and proliferation in melanocytes [135]. MC1R is expressed in most UM [136] and has been targeted using an MC1R-ligand based radiopharmaceutical. [225]Ac-DOTA-MC1RL showed MC1R-specific cytotoxic *in vivo* reducing both tumor growth and metastatic burden in Mel270-xenografts [137]. More recently, inhibitors are being developed to selectively inhibit Gαq[mut] proteins. In total, 3 Gαq-inhibitors have been tested *in vivo.* The development of Gαq-inhibitors is an ongoing field where chemical adaptations improve efficacy. From the *in vivo* studied Gαq-inhibitors, FR900359 and GQ127 inhibited tumor growth in Gαq/11[mut]-xenografts (MP41, MP46) by repression of pERK or YAP while Gαq[WT]-xenografts (OCM-1 A) remained unaffected [138–140]. Recently the first combined treatment with a selective Gαq-inhibitor study described synergistic effects with an Insulin-like growth factor 1 receptor (IGF1R) inhibitor [141]. The IGF1R pathway involves activation of Insulin-like substrate 1/2 (IRS1/2), which upon inhibition alters the PI3K-AKT pathway in UM xenograft models [142]. The IGF1R pathway has been described as a potential resistance mechanism for metastatic UM [143], as IGF1 is secreted by liver cells [144]. In a hepatic xenograft model using UM001 cells, Gαq/11-inhibitor YM-254890 did not inhibit tumor growth; yet when combined with IGF1R-inhibitor the treated mice exhibited a significant decrease in tumor volume [143]. These results further support the idea that liver-secreted molecules are involved in metastatic disease and compound resistance. The latest Gαq-inhibitor, GQ262, showed many improvements compared to its predecessor GQ127; holding an increased metabolic and oxidative stability with a longer half-life time. But most noteworthy was the ability of GQ262 to elucidate a dose-depended response where some mice had complete remission [145].

Targeting GPCRs remain a valid option with strong responses *in vivo,*

although CXCR4 expression holds discrepancies in the literature, CXCR4 antagonists and MSX-122 illustrated their effective inhibitory abilities against CXCR4[positive] UM-cells *in vivo*. Patients that hold high expression of CXCR4 could benefit from these compounds, yet these compounds need to be studied in more detail as their effectiveness has only been shown in the OMM2.3 cell line. The ongoing development of Gαq-inhibitors might hold the most promising results for the majority of UM patients. Complete remission, even *in vivo,* has only been described in two reports [104,145], making GQ262 one of the most promising targeted therapeutics regardless of secondary mutation.

3.3.4. Inhibiting common cancer pathways in UM murine xenografts

Development and progression of cancer harbour multiple hallmarks, including resistance to cell death, sustained proliferation, inducing angiogenesis and activating invasion and metastasis [111]. Targeting hallmarks of cancer can provide effective treatment options and have been widely studied in UM xenografts. In the field of oncology, chemotherapy is usually the initial treatment choice, and it works by causing DNA damage, which in turn triggers the activation of pro-apoptotic factors [146], however as discussed above targeting DNA alone has poor response in UM patients [39]. Combining chemotherapy with compounds that target DNA-repair genes improved apoptosis-signalling *in vivo* [119,147]. Interestingly, targeting anti-apoptosis proteins without additional chemotherapy is able to reverse cellular state from resisting cell death towards active apoptosis *in vivo* by themselves (Fig. 3, supplementary table 3) [148,149]. Besides inducing apoptosis, halting proliferation is equally important to inhibit tumor progression. Important proteins in mitotic progression, DNA replication and cell cycle entry are Cyclin-dependent kinases (CDKs) [150]. By inhibiting proteins involved in cell cycle entry and DNA replication, such as SKP2, CDK4 and CDK6, UM growth is effectively inhibited *in vivo* [151,152]. Combining a CDK4/6 inhibitor with a MET inhibitor improves treatment effectivity by not only reducing tumor growth, but also inhibiting metastasis [153]. However, it seems that targeting CDK2, CDK7 and CDK9 should be preferred as potential treatment as *in vivo* models demonstrated reduced tumor growth and lower metastatic

burden using a single compound (Fig. 3, Supplementary table 3) [154]. In order for tumor cells to keep proliferating, access to nutrients is essential. Tumor cells are able to secrete proangiogenic factors to induce sprouting of new blood vessels to sustain neoplastic growth. Additionally, this provides tumor cells access to the circulatory system in which they can invade for distant metastasis [111]. Inhibition of proangiogenic factors in UM xenografts illustrated strong effectivity in reducing both tumor growth and metastatic burden [155,156]. As most cancer related deaths are due to metastasis [157], mechanisms driving these events are suitable targets to inhibit or prevent metastatic disease. A well-known signalling pathway driving metastasis in many cancers is the NF-κB-pathway. NF-κB has been linked to regulate cancer stem cells, epithelial-to-mesechymal transition (EMT), pro-proliferation and anti-apoptotic genes, angiogenesis, adhesion molecules and secretion of matrix met-alloproteases [158]. NF-κB is expressed in primary UM and elevated in their corresponding metastasis [159]. Several compounds inhibiting the NF-κB-pathway have been studied in UM xenografts (Supplementary table 3). The treatment outcome differs per compound used, as some NF-κB-inhibitors reduced tumor growth [160,161] while others also inhibited metastatic burden [162–164]. Rather than concentrating on well-known metastasis-related pathways, it is perhaps more compelling to explore specific pathways and their regulatory networks in uveal melanoma (UM).Due to the clear correlation between secondary drivers and the likelihood of metastasis [11,19]. Sub-dividing UM based on secondary mutation illustrated distinct gene expression profiles, which suggests high- and low-risk UM utilizes different molecular pathways [165]. Gene expression profiles of high-risk UM illustrate a loss of melanocytic differentiation [166], which is thought to be regulated by histone deacetylases (HDACs) [167]. HDACs are important epigenetic regulators of gene expression and are involved in cancer initiation and progression [168]. HDAC inhibition reversed the dedifferentiated state of _BAP1_-deficient cells towards a more melanocytic gene expression profile _in vitro_ and reduced tumor growth in a 92.1-xenograft model [167]. HDAC inhibitor Quisinostat demonstrates selective efficiency on _BAP1^mut_ UM cells (MP46, MM28) as _BAP1^wt_ cells (MP41) remain unaffected [169]. However, not all HDAC inhibitors seem to be specific per secondary mutation profile as HDAC inhibitor JSL-1 was able to inhibit _BAP1^WT_ tumor growth _in vivo_ [170]. Additionally, the question remains if HDAC inhibitors are really specific against certain subtypes, as HDAC inhibitors have been shown to be effective in other cancers that harbour _SF3B1_- (colorectal carcinoma) or _BAP1_-mutations (mesothelioma) [171,172]. Another class of gene regulatory proteins are Bromodomain and extra-terminal domain (BET) proteins. BET regulate gene expression by chromatin remodeling and histone modifications [173]. BETs have been associated with regulating genes involved in tumorigenesis such as MYC proto-oncogene, bHLH transcription factor (_MYC_) while also regulating metastatic pathways such _via NF-κB_ [174]. _MYC_ is located on chromosome 8q, a locus which is frequently amplified in high-risk UM [175], which can selectively be inhibited by BET inhibitor JQ1 [176]. JQ1 treatment in 92.1-xenografts inhibited tumor growth, however _in vitro_ studies showed JQ1 is unable to inhibit Gαq^WT cells (Mel290); suggesting BET inhibitors efficiency could depend on driver mutation status [177]. BRD4, a member of the BET protein family, has been shown to regulate YAP expression in UM. Inhibiting BRD4 showed reduced tumor growth in both mice and zebrafish [178]. Together, it seems BET inhibitors are promising for Gαq^mut UM, but not for Gαq^WT UM. Inhibition of BET proteins gained interest in various cancer fields, which led to several clinical trials. However, it became evident that resistance to BET inhibitors was gained _via_ different mechanisms, seen by unaltered MYC expression despite globally reduced BRD4 or _via_ WNT-signalling activation [179,180]. UM cells resistant to BET inhibitors can be sensitised to treatment by a second compound. These methods reduced tumor volume _in vivo_ by adding a NF-κB inhibitor [181] or _via_ targeting the microenvironment due to inhibition of Fibroblast Growth Factor Receptors (FGFR) [182].

Summarizing, many compounds have been evaluated _in vivo_ with promising results. Yet, due to the wide variety of cell lines used to generate these models, translatability is difficult. (Tables 1–3 and supplementary table 3). Additionally, most efforts have been targeted towards driver mutation activating MEK1/2 or AKT-PI3K-mTOR signalling (Fig. 3) that inhibit tumor growth but in general fail to achieve complete remission. Most evidence to inhibit metastasis is seen after inhibiting angiogenesis, NF-κB or cyclin-dependent kinases; however, these compounds were evaluated in BAP^WT-xenografts that lack the typical pathogenesis seen in UM patients. While targeting BET is a promising strategy to inhibit Gαq^MUT-UM, there is evidence of resistance against BET inhibitors. Therefore, alternative strategies may offer quicker and more effective results. Notably, there are 2 compounds that have been reported to exhibit signs of achieving complete remission: Withaferin A and GQ262 (Fig. 4). These compounds hold promising results, but should be validated in multiple experiments such as in _BAP1^mut_-xenografts and metastatic models (_e.g._ splenic inoculation based xenografts).

3.4. Antibody-based therapy and oncolytic virotherapy

In comparison with pharmaceutical inhibition, antibody- and viral-based inhibition is much less studied in UM, despite the success stories in cutaneous melanoma. In our structured literature search only 2 molecules have been targeted using monoclonal antibodies and 5 molecules with viral transduction in Gαq^mut UM cells (Table 4). Immune-modulation could provide novel strategies as for instance high-risk UM harbour more HLA I and II surface markers which induce a pro-tumorigenic immune landscape [183]. An overview of the used antibodies, viruses and cell lines and compound effects can be seen in Fig. 5 and Table 4.

3.4.1. Antibody-based therapy
The first monoclonal antibody tested UM xenograft models targeted gangliosides, a membrane bound molecule found on melanoma cells. However, _in vivo_ experiments in this study were evaluated with OCM melanoma cell lines (BRAF^mut) as Mel202 cells had a very low amount of ganglioside expression [184]. The first antibody based treatment against Gαq/11^mut UM cells (92.1) targeted Epidermal growth factor receptor (_EGFR_), which is able to induce cell-lysis in EGFR^positive UM cells _in vitro_. Expression of EGFR in UM was correlated to increased liver metastasis, while inhibiting EGFR-signalling improved overall survival and reduces the severity of liver metastasis in 92.1-xenografts [48]. Similar to pharmaceutical studies, inhibition of angiogenesis has also been studied using monoclonal antibodies. Targeting _Vascular endothelial growth factor_ (VEGF), proliferation and invasive capacity were inhibited _in vitro_, and reduced the number of micro metastasis in Mel290-xenografts [49]. More recently, a novel cell surface molecule, melanoma cell adhesion molecule (MUC18), was identified using a nanobody library screen in Gαq/11^mut-UM cells (MP41, MM33) [185]. Inhibition of MUC18, either _via_ monoclonal antibody or siRNA, resulted in inhibition of several mechanisms that activate angiogenesis and vasculogenic mimicry. However, this study used SP6.5 cells (BRAF^mut) which impairs translation to Gαq/11^mut-UM biology [186]. Although only 2 antibody-based strategies have been reported in Gαq/11^mut-xenografts, both were able to inhibit metastasis. Interestingly, inhibiting angiogenesis has been reported to inhibit metastasis in UM xenografts using either antibodies and chemical compounds.

3.4.2. Oncolytic virotherapy
Oncolytic virotherapy uses viruses or viral-like particles to induce specific tumor targeting and subsequent aim to stimulate cell death [187]. A total of 5 studies investigated different types of virotherapy in _Gαq/11^mut_ UM-xenografts and 1 study using a _Gαq/11^WT_-model (Table 4). The first known study used canary pox virus expressing human gp100 to generate HLA-A:0201+ cytotoxic T-lymphocytes (CTLs) _in vivo_ that specifically target human-gp100 epitopes [188].
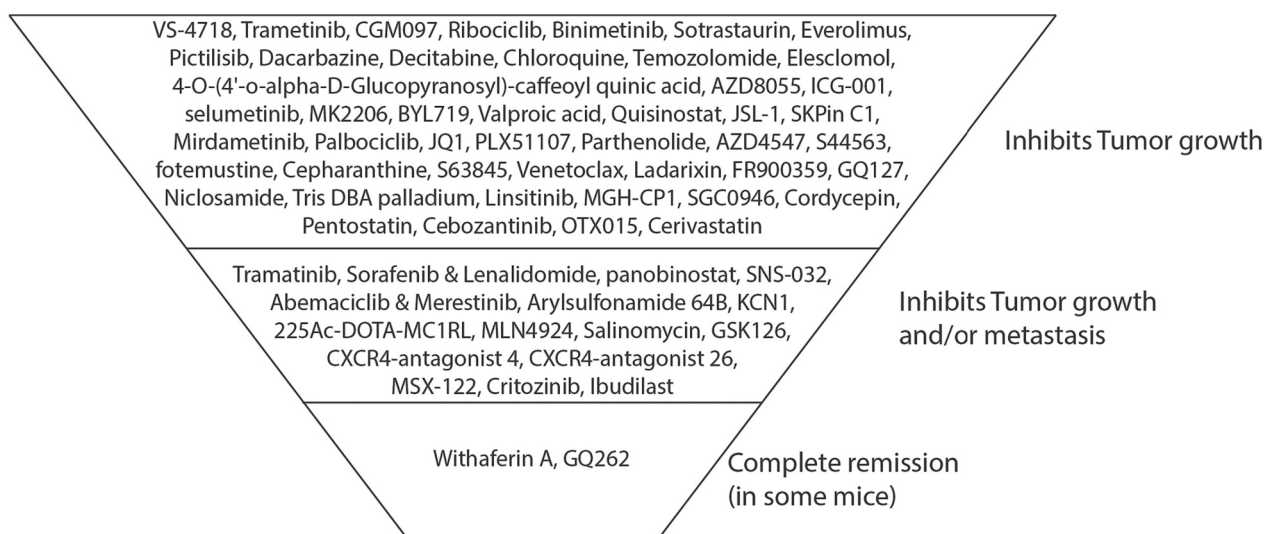
Fig. 4. Funnel Chart of compounds evaluated in UM xenografts. The majority of compounds only inhibited tumor growth, others inhibited metastasis and a couple compounds inhibited both. Only 2 compounds showed complete remission in a few mouse models.

Table 4
Overview of antibodies and viruses used for therapeutic intervention in UM xenografts. For each study the cell line used to generate xenografts is shown with the type of intervention followed by the corresponding effect after treatment.

Antibody-Based therapy

Target	Dose (in μg)	Administration	Type	Cell line	Effect	Ref.
GD2	200	Single dose	monoclonal anitbody	OCM1	Reduced metastasis	[184]
EGFR	250	Single Dose	monoclonal anitbody	92.1	Reduced liver metastasis	[48]
VEGF	250	Single dose or 2 times per week	monoclonal anitbody	Mel290	Reduced proliferation, invasiveness and liver metastasis	[49]
MUC18	–	–	nanobody	MP41, MM33	Identification	[185]
MUC18	4	Single Dose	Monoclonal antibody	SP6.5	Reduced tumor growth	[186]

Oncolytic virotherapy

Target	Dose	Administration	Type	Cell line	Effect	Ref.
gp100	(Adoptive T-cell transfer)	–	canarypox virus	OMM1	Complete tumor eradication	[188]
HSPG	100 or 200 μg	Single dose	Virus Like Particle-conjugate	92.1	Induces cell death	[190]
CREB, HIF-1	(Injected cells contained virus before inoculation)	–	Retrovirus	Mel270	Reduced tumor growth	[192]
Immune-landscape	1×10^5 PFU/μl	Single dose	Herpus simplex virus type 1	92.1	Reduced tumor growth	[193]

Many uveal melanomas express gp100 on their membrane [189], making it an interesting target for immunotherapy. *Via* intraocular inoculation of UM cells (OMM1), this study was the first to show CTLs are able to infiltrate the immune-privileged structures of the eye with the capacity to induce cell death. *Via* adoptive transfer of HLA-A:0201-gp100+ CTLs from mice into immunocompetent mice harbouring human UM cells (OMM1) the authors achieved complete eradication of the tumor without immunopathological damage to the eye [188]. It is interesting to note that treatment in UM using tebentafusp, which also modulates CTLs to target gp100, is the first immunotherapy that shows a significant response in patients [22].

Instead of modulating immune-cells, other have tried to induce viral-based cell death. A viral-like particle, which can bind to cell surface heparin sulphate proteoglycans (HSPG), was conjugated with phthalocyanine photosensitizer IDRye700DX (together called AU-011). Infrared waves can activate AU-011 to release its cytotoxic properties and become active intracellularly. *In vivo* treatment with AU-011 showed a dose-dependent response after emission of infrared waves, activating AU-011 which induced cell death in 92.1-xenografts [190].

Another approach utilized retroviruses as drug-carriers to infect tumor cells and release their cytotoxic compounds. The transduction of retroviruses relies on dividing cells [191] and consequently they tend to infiltrate highly proliferating cells, enabling the selective targeting of tumor cells. Retroviruses armed with shRNA against pro-angiogenic factors *HIF1* and *CREB* halted tumor growth in Mel270-xenografts, where *CREB* inhibition was most potent [192]. The latest study evaluated herpes simplex 1 virus (HSV-1), an approved oncolytic virus by the FDA, for UM treatment [193]. Infection of HSV-1:EGFP significantly reduced tumor volume in 92.1-xenografts by inducing the release of cytokines. This was due to an increase of interferon gamma recruited anti-tumorigenic macrophages, NK cells and mature dendritic cells to inoculation site [193]. The presence of for instance NK cells in peritumoral regions was known to being able to induce cytolysis of UM cells depending on their MHC-class back in 1995 [194], providing further evidence anti-tumorigenic immune-landscape could be utilized for UM treatment.

3.5. Zebrafish uveal melanoma xenograft models

The zebrafish (*Danio rerio*) has proven itself to be a powerful vertebrate cancer model system with multiple advantages such as, high number of offspring, ex utero development, ease of genetic manipulation through one-cell stage microinjections, relatively cheap maintenance, availability to generate patient derived xenograft models, stable
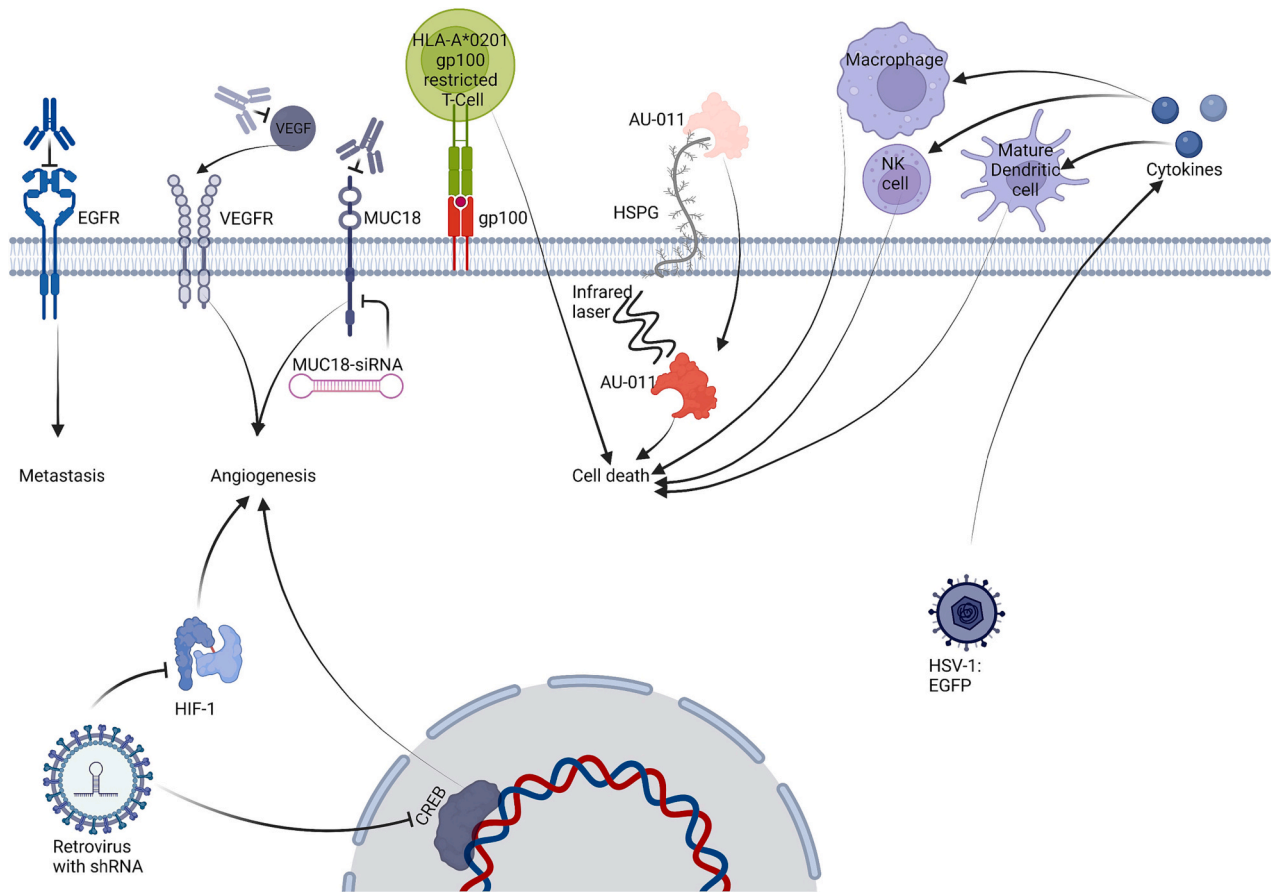
Fig. 5. Schematic overview of antibody-based or oncolytic virotherapy used in xenograft UM mouse models. Antibodies targeting receptors or ligands are illustrated in similar colour. Abbriviations: Epidermal growth factor receptor (EGFR), Vascular endothelial growth factor (VEGF), melanoma cell adhesion molecule (MUC18), hypoxia inducible factor 1 subunit alpha (HIF-1), premelanosome protein (gp100), Heparan sulfate proteoglycan (HSPG), Herpes simplex virus 1: enhanced green fluorescent protein (HSV-1:EGFP). (For interpretation of the references to colour in this figure legend, the reader is referred to the web version of this article.)

Table 5

Overview of compounds studied in UM xenograft zebrafish models. For each study the used cell line used to generate xenografts are shown with the corresponding compound effect after treatment. Abbreviations: histone deacytelyase (HDAC), Nuclear factor kappa-light-chain-enhancer of activated B cells (NF-κB), MET proto-oncogene, receptor tyrosine kinase (MET), cysteinyl leukotriene receptor 1 (CYSLTR1), reactive oxygen species (ROS), deoxynucleic acid (DNA), melanocyte inducing transcription factor (MITF).

Xenograft zebrafish models						
Drug	Target	Dosage	Therapy	Cell line	Compound effect	Ref.
Dasatinib	Src tyrosine kinase	4 μM	Single			
Quisinostat	HDAC	0,125 μM, 2,5 μM	Single	Mel270, 92.1, OMM1, OMM2.3, OMM2.5	Reduced tumor burden, reduced tumor cell dissemination	[202]
MLN-4924	NF-κB	1 μM	Single			
Crizotinib	MET	5 μM	Single	92.1, OMM2.5	Reduced tumor burden, reduced tumor cell dissemination	[205]
quininib	CYSLTR1	3 μM	Single			
1,4-dihydroxy quininib	CYSLTR1	10 μM	Single	Mel285, OMM2.3	Reduced tumor burden	[207]
montelukast	Immune-modulation	20 μM	Single			
Carbon dots	ROS	25-200μg/ml	Single	92.1	Increased tumor burden	[208]
Dacarbazine	DNA	20 μM	Single			
Ricolinostat	HDAC	20 μM	Single	OMM2.5	Reduced tumor burden (Dacarbazine not effective)	[206]
ML329	MITF	1.25 μM	Single			
Navitoclax	BCL-2	0.625 μM	Dual	spUM-LB008	Reduced tumor burden	[209]
everolimus	mTOR	0.625 μM				
Everolimus	mTOR	2.5 μM				
Nacitoclax	BCL-2	2.5 μM				
Quisinostat	HDAC	0.5 μM	Dual	spXmm66	Reduced tumor burden	[210]
Sotrastaurin	PKC	2.5 μM				
Flavopiridol	CDK9	1.0 μM				

expressing transgenic lines [195], a large genetic toolbox [196] and extensive conserved organ-specific genetic programming and cancer-associated genes with humans [197]. The use of zebrafish models in cancer research has increased in the last decade [41,198]. Due to the increased interest, an online deposit has been generated for researchers to share data on zebrafish larval xenografts [41].

3.6. Pharmacological studies in zebrafish uveal melanoma xenografts

Transplantation of tumor cells in zebrafish larvae are achieved by simple microinjection of tumor cells. Engraftment of tumor cells is very high as zebrafish larvae lack a mature adaptive immune system [199]. A major advantage of xenografts in zebrafish larvae is their transparent development [200], which allows for fluorescent tracking of tumor cells. Using a reporter line with fluorescent blood vessels, interaction between tumor cells and surrounding vasculature can be studied in detail [201]. Using this advantageous method, xenograft models of cutaneous and uveal melanoma illustrated that extrusion from blood vessel where morphologically distinct from each other [201]. Multiple UM cell lines have been have been successfully transplanted into zebrafish larvae and illustrated tumor growth and metastatic potential that correspond to human disease progression [202].

An major advantage this model holds is the potential for large compound screening due to the large amount of offspring [203]. Compounds are screened by adding compounds in growth medium, which is subsequently taken up by zebrafish larvae through their gills or skin [204]. An overview of compounds evaluated in UM zebrafish xenografts are summarized in Table 5. Reports of UM xenografts in zebrafish larvae date back to 2014. Primary (92.1, Mel270) and metastatic (OMM1, OMM2.3, OMM2.5) UM cell lines were able to be engrafted, and showed proliferation and dissemination within 6 days post injection. Inhibition of HDACs, NF-κB [202] or MET [205] showed reduction in tumor burden and migration in these models; which was also seen in mice [124,169]. Additionally, zebrafish xenografts have also illustrated their potential to identify novel compounds inhibiting UM. Inhibition of HDACs by Ricolinostat reduced tumor burden in OMM2.5-xenografts due to transcriptional loss of *Melanocyte Inducing Transcription Factor (MITF), SRY-box Transcription Factor 10 (SOX10), Melanophilin (MLPH) and Dopachrome Tautomerase (DCT)* [206]. Reduction of tumor burden was also seen after inhibiting Cysteinyl Leukotriene Receptor 1 (CYSLTR1, a GPCR frequently amplified in high-risk UM) in primary (Mel285) and metastatic (OMM2.5) UM-xenografts. CYSLTR1 inhibition did not alter the migration behaviour seen in these models [207]. Zebrafish xenograft treated with carbon dots, which induces ROS, exhibited increased tumor burden suggesting ROS-inhibition could potentially hold therapeutic options for UM [208]. These results are in discordance with a mouse model where elesclomol, a copper-based ROS inducer, inhibited tumor growth despite both using 92.1-xenograft models [115]. Most recent development in zebrafish UM xenografts demonstrated their ability to perform fast drug screening in patient-derived xenografts. By generating spheroids of patient tissue, implantation in zebrafish larvae and subsequent treatment of a mTOR and BCL-2 inhibitor; this model demonstrated their versatility as a pre-clinical model as these compounds significantly reduced tumor burden in a similar fashion as seen in mouse models [209]. This system was subsequently used to screen compounds in many patient-derived spheroids, which illustrated spheroid-based xenografts hold a higher amount of tumor burden compared to adhered cell culture-based xenografts and a more sensitive assessment of compounds as combinations attempted in mouse models failed but were successful in this system [210].

Next to drug-screening, zebrafish models can also be utilized to investigate genetic effects on tumor cells. Secondary driver mutations in UM are mutually exclusive, however why this is the case remains largely unknown. To gain insight into why UM does not acquire other secondary driver mutations that could be beneficial, *SF3B1^{mut}* cells were studied after knocking out *BAP1 via* CRISPR-Cas9 technology. *In vitro* results

showed these cells lack functional DNA repair mechanisms and eventually went into senescence. Their lack of activity was validated in zebrafish as these cells migrate to a significant lower extent, suggesting acquiring both *SF3B1^{mut}* and *BAP1^{mut}* are not advantageous for UM cells [211]. Although xenograft studies are a rapid and powerful system to evaluate candidate compounds, the lack of an adaptive immune system in zebrafish and the use of human cancer cell lines are disadvantages. Yet compared to mice, the data is equally valuable and show similar results when the same compound is studied. Considering the ease and cost-effectiveness using the zebrafish larvae, this model could improve and accelerate compound development for UM.

3.7. Clinical trials which have pre-clinical evidence of xenograft models

After extracting all clinical trials of uveal melanoma which reported results in https://www.clinicaltrials.gov/, 36 trials out of 220 (Supplementary table 4) were used to evaluate the use of pre-clinical evidence reported by xenograft models. To our surprise, only 3 clinical trials used compounds that have been tested *in vivo,* where only 1 trial published results (Table 6). Xenograft models illustrated a reduction of tumor growth *via* an observed synergistic effect by inhibiting PKC and MEK by Sostrastaurin and Binimetib [99,103]. Yet in clinical trials, this synergistic effect was not seen in patients, however there was a higher degree of stable disease compared to dacarbazine treatment. The authors stated that due to substantial gastrointestinal toxicity seen in patients the trial had to be stopped and they have no plans for future clinical trials to continue. So far, there is no trial with reported results that have utilized zebrafish xenograft pre-clinical data.

4. Transgenic uveal melanoma models

Transgenic cancer models are preferred over xenograft based models as these models are immunocompetent, follow more closely the natural history of tumor development and metastatic processes [213]. Additionally, transgenic models are not hampered by histoincompatibility between donor and host cells [214]. However, generating transgenic models with cell specific tumors and compatible disease genetics as seen in humans is complex and difficult to achieve.

4.1. Transgenic uveal melanoma models in mice

Since 1991, transgenic mice have been generated where the typical approach was using melanocyte-specific promotor, *Tyrosinase,* that drives a simian virus 40 (SV40) transgene (Tyr-SV40E mice) [215]. In C57Bl/6 mice this method generated early ocular melanoma and later in life developed subsequent mucosal and cutaneous melanoma [215]. While the tumors exhibited invasiveness both into both local and distant organs, liver metastasis were notably absent [216].

Others used the same transgenic construction, but expressed transgenes in an albino mouse strain (FVB/N mice). In this modified mouse strain, expression is restricted to the retinal pigment epithelia (RPE) and these mice developed ocular tumors, however these tumors are not invasive. Only after extraction and subsequent transplantation of transgenic tumors into nude mice, liver metastasis were present [217]. Subsequent models based on SV40 oncogenic potential were adapted to express *SV40 T antigens* (*Tag*) driven by the *Tyrosinase* promotor (Tyr-Tag mice) or *Tyrosine like protein 1 (Tyrp1)* promotor (Table 7). SV40 T antigens driven by *Tyrp1* developed spontaneous RPE tumors [218,219], whereas *Tyr*-driven models developed bilateral ocular melanoma with expression of HMB45 and Fas-ligand; markers that were lacking in tg (Tyr-SV40E) mice [220]. Tyr-Tag mice were used to evaluated novel treatment using 1α-Hydroxyvitamin D2 [221] and TSP1-mimetic anti-angiogenic peptide [222], which both inhibited tumor growth but were unable to provide complete remission. Additionally, Tyr-tag mice has been utilized to illustrate causal gene switches between class 1 UM and class 2 UM. Gene expression analysis of human UM identified loss of

Table 6

Clinical trials with reported results that have utilized pre-clinical data from mouse xenograft models.

Mouse xenograft model	Ref.	Clinical Trials with Results	Clinical Trial number	Effect	Ref.
Sostrastaurin, Binimetib	[99,103]	Sostrataurin, Binimetib	NCT01801358	No synergystic effect observed in patients. Treatment associated with substantial gastrointestinal toxicity.	[212]
Bevacizumab	[49]	Ozurdex or Bevacizumab	NCT01471054	Not enough patients	NA
gp100 vaccine	[188]	mouse gp100 plasmid DNA vaccine	NCT00398073	No publication	NA

Inhibitor Of DNA Binding 2 (*ID2*) expression in class 2 UM compared to class 1 UM. Expressing the Tyr-Tag construct in *Id2*$^{-/-}$ mice altered tumor morphology and presented a higher mitotic index [223].

Transgenic tumor models have also been developed with mutant *HRas Proto-Oncogene, GTPase* (*HRAS*). *Tyrosinase* driven-T24 *Ha-Ras* in mice (TP-ras mice) spontaneously develops hyperpigmentation and melanocytic hyperplasia at 13 weeks of age [224], which was faster than Transforming growth factor alpha (TGFα) -based transgenic model [225]. A time dependent study showed most TP-ras mice harbour melanocytic/RPE proliferation early in life, but could also develop uveal melanoma later in life [226]. Crossing TP-ras mice with *lnk4a/Arf*$^{-/-}$ mice (these mice lack a tumor suppressor locus) resulted in a higher abundancy of uveal melanoma, but also harbour a high number of cutaneous melanoma [227]. The TP-ras;*lnk4a/Arf*$^{-/-}$ model was subsequently used to investigate immune-modulation *via* a yeast-based vaccine. Administration of whole recombinant yeast expressing human *MART-1* induces a Th1-specific cytokine release which recruited CD4+ and CD8+ T-cells to the melanoma and exhibited active cytotoxicity [228]. However, TP-ras;*lnk4a/Arf*$^{-/-}$ mice that expressed a mice *Melanoma antigen gene* (*MAGE*) -type antigens were resistance against tumor infiltrating lymphocytes *via* the Fas/Fas-ligand axis [229], suggesting the type of antigen expressed on the membrane is crucial to develop targeted therapies.

Next to the *SV40* and *HRAS* based models, melanomas were also induced *via glutamate receptor 1* (*GRM1*) [230], *KRAS* [231], hepatocyte-growth factor overexpressing mice [232], and *Ret Proto-Oncogene* (*RET*) [233–239]. However, these models are all based on genes which are typically not seen human UM. A total of 5 transgenic mouse models have been described using *GNAQ*^{mut} or *GNA11*^{mut} as transgenes to drive UM in mice. The majority are *GNAQ*^{Q209L}-driven models (4/5) that rely on conditional expression *via* CreERT- or TetOn-based activation. The first described Gαq-based model used the TetOn-based conditional expression where *GNAQ*^{Q209L} expression is induced in a melanocyte specific manner *via* the regulatory elements of *DCT*. Although, no uveal melanomas were described, this model did help to identify YAP and the Hippo pathway involvement in melanocytic neoplasms [66]. The other 3 models located *GNAQ*^{Q209L} in the *Rosa26* locus with *Loxp*-sites, where expression was achieved *via* CreERT that is driven by melanocyte-specific promotors (*Mitf*-, *Tyr*- or *Plp1*-promotor). Induction of *GNAQ*^{Q209L} expression *via Mitf*-Cre resulted in cutaneous nevi, melanocytoma of the central nervous system (CNS) and UM [240–242]. This model developed invasive melanoma, as metastatic lesions were present in the lung [242] and showcased the role of *Endothelin Receptor Type B* (*Ednrb*) in tumorigenesis [240]. Interestingly, *Tyr*-Cre and *Plp1*-Cre based induction did not form UM, but did induce melanocytomas of the CNS, whereas Tyr-Cre activation caused cutaneous, CNS and uveal melanocytic neoplasms [242]. Combining *GNA11*^{Q209L} with *Bap1* loss did not increase malignancy but rather showed slimmer neoplasms. A possible explanation was that the *GNA11*^{Q209L}:*Bap1*$^{-/-}$ mice had a shorter survival due to increased skin melanoma burden [243]. This model (as in the other Gαq/11-based models) did not show liver metastasis. Nonetheless, these models proved their potential to study tumorigenesis in primary UM, per example this model system identified *RasGRP3* as an important node in Gαq/11-signalling [243]. Despite the many efforts to generate tissue-specific transgenic UM mouse models,

the current models struggle with restricting expression of oncogenes to ocular melanocytes. Additionally, liver metastases have nog been described in these models; which are crucial to obtain a model that truly reflect human disease progression.

4.2. Transgenic models in zebrafish

The zebrafish community has put a lot of effort in identifying tissue-specific promotors [244]. Using these promotors allows for tissue-restricted expression of a gene of interest. Transgenic UM zebrafish models so far have been generated utilizing the melanocyte-specific promotor *mitfa* (Table 8). The first UM transgenic fish model was made in medaka where Xiphophorus melanoma receptor kinase (*Xmrk,* a mutated EGFR) was expressed under the control of *mitf*. These fish developed melanomas in the skin, eye and CNS [245,246]. Six years later, the first zebrafish model was described where human *GNAQ*^{Q209P} was expressed in melanocytes. Although choroidal hyperplasia was seen in tg(GNAQ^{Q209P}) zebrafish, to acquire melanomas loss of *tumor protein p53* (*tp53*) was necessary [247]. The fact that *GNAQ*^{Q209P} is not enough to induce tumors is interesting as in humans Gαq/11-mutations are seen in blue nevi, which typically are not aggressive [53]. In contrary, *GNAQ*^{Q209L} in mouse melanocytes are sufficient to from melanomas [99], suggestive that zebrafish might recapitulate the natural history of UM more closely. Furthermore, transgenic zebrafish harbouring *GNAQ*^{Q209L} and *GNA11*^{Q209L} in *tp53*-deficient zebrafish acquired mainly skin melanomas and only a small number of ocular tumors [248].

Studies on other driver mutations (in *CYSTLR2* and *PLCB4*) or downstream effectors (*YAP*) in zebrafish melanocytes were sufficient to induce tumor formation in combination with loss of *tp53*, confirming their oncogenic capacity. However, as seen in transgenic mice, these models do not show liver metastasis despite having an invasive behaviour to surrounding tissue [249]. The transgenic UM models in zebrafish struggle to achieve tissue-specificity. Furthermore, in order to form malignancies, these models rely on *p53* loss; which is typically not altered in UM. There are no transgenic lines that combine driver mutations with known secondary mutations (*EIF1 AX, SF3B1* or *BAP1*), which would be of interest as these might allow for melanomas to form without the need to alter *p53*.

5. Discussion and considerations

For over 40 years the field has tried to generate representative UM models. Even though, much is learned from these models, current models are often inadequate and do not replicate the natural progression of the disease as seen in humans. After in-depth literature screening, *circa* half of the publications contained animal models generated with non-human cells or with *BRAF*- or *NRAS*-mutated melanoma cell lines (Fig. 1A). These mutations are typical for cutaneous melanoma [42], and were therefore not included in this review as these do not represent typical UM biology. For generating xenograft UM mouse models, subcutaneous inoculation was the most frequently used site (Fig. 1B). The microenvironment of tumors is an important element in their evolution and progression [252], therefore intra-ocular (*e.g.* choroidal) inoculations should be considered in future xenograft models. Intra-ocular inoculation will present a more natural environment of UM, and others

Table 7

Overview of transgenic models that spontaneously develop melanoma's. The name used to describe the transgenic line are shown together with the mouse strain used, which promotor is driving transgenic expression and which transgene was utilized for oncogenic potency.

Mouse name	Mouse Strain	Promotor	Transgene	Ref.
Dct/HA-GαqQL/p16p19^{KO}	FVB/N	Dct	$Gnaq^{Q209L}$	[66]
Ric-8Aflox.flox	C57Bl/6	Rosa-Cre	$Ric8a$ deletion	[61]
tg(Tyr-SV40E)	C57BL/6	tyrosinase	$SV40$	[215]
tg(Tyr-SV40E)	C57BL/6	tyrosinase	$SV40$	[216]
tg(Tyr-SV40E)	FVB/N	tyrosinase	$SV40$	[217]
Tyr-Tag	CB6F1	tyrosinase	$SV40\ t$ antigens	[220]
Tyr-Tag	CB6F1	tyrosinase	$SV40\ t$ antigens	[221]
Tyr-Tag	CB6F1	tyrosinase	$SV40\ t$ antigens	[222]
Tyr-Tag; $ld2^{-/-}$	CB6F1	tyrosinase	$SV40\ t$ antigens	[223]
Tyrp1-Tag	NMRI/Han	tyrosinase like protein 1	$SV40\ t$ antigens	[218]
Tyrp1-Tag	NMRI/Han	tyrosinase like protein 1	$SV40\ t$ antigens	[219]
TP-ras	C57BL/6 J x SJL/J and C57B/6 x CBA	tyrosinase	$T24\ Ha\text{-}ras$	[224]
Tyr-TGFa	NMRI/Han	tyrosinase	$Tumor$ $growth\ factor$ $alpha$	[225]
TP-ras	C57BL/6XSJL X C3He/N	tyrosinase	$T24\ Ha\text{-}ras$	[226]
Tyr-RAS; + link4a/ARF$^{-/-}$	FVB/N	tyrosinase	$T24\ Ha\text{-}ras$	[227]
Tyr-RAS; + link4a/ARF$^{-/-}$	FVB/N	tyrosinase	$T24\ Ha\text{-}ras$	[228]
TiRP	B10·D2	tyrosinase	$H\text{-}Ras,$ $Trap1a$	[229]
Tg(Grm1)Epv	C57Bl/6	Dct	$glutamate$ $receptor\ 1$	[230]
Lats1$^{fl/fl}$;lats2$^{fl/fl}$, yap^{fl}, taz^{fl}	CFW	AAD;Cre	$Kras$	[231]
HPN	HP mice with Nme1$^{-/-}$; Nme2$^{-/-}$	–	–	[232]
F1.RET	NOD Nos2$^{-/-}$	metallothionein-I	ret	[233]
RET.AAD	C57Bl/6	metallothionein-I	ret	[234]
RET.AAD	C57Bl/6	metallothionein-I	ret	[235]
RET.AAD	C57Bl/6	metallothionein-I	ret	[236]
RET.AAD	C57Bl/6	metallothionein-I	ret	[237]
ret-transgenic	C57Bl/6	metallothionein-I	ret	[238]
RET.AAD	C57Bl/6	metallothionein-I	ret	[239]
Rosa26-fs-GNAQ^{Q209L}; Ednrb$^{Flox/flox}$	C57BL/6 × 129/SvEv	Mitf-cre, tyr-cre, Plp1-cre	$GNAQ^{Q209L}$	[240]
Rosa26-fs-GNAQ^{Q209L}	C57BL/6 × 129/SvEv	Mitf-cre, tyr-cre, Plp1-cre	$GNAQ^{Q209L}$	[241]
Rosa26-fs-GNAQ^{Q209L}	C57BL/6 × 129/SvEv	Mitf-cre, tyr-cre	$GNAQ^{Q209L}$	[242]
Rosa26-fs-GNAQ^{Q209L}	C57BL/6 J	tyrosinase	$GNA11$ or $Bap1^{-/-}$	[243]

Table 8

Overview of transgenic UM zebrafish. For each study the strain of fish with their genetic background are shown together with the promotor that drives the corresponding oncogene.

Transgenic zebrafish lines				
Fish	Fish strains	Promotor	Transgene	Ref.
Oryzias latipes	Carbio, Albino, tp53$^{-/-}$	mitf	xmrk	[246]
Danio rerio	Wild-type (AB?), Golden	mitfa	GNAQ^{Q209P}, BRAF^{V600E}, NRAS^{Q61L}	[247]
Danio rerio	WT (AB?)	mitfa	GNA11^{Q209L}, GNA11^{R183C}	[250]
Danio rerio	tp53$^{-/-}$	mitfa	GNAQ^{Q209L}, GNA11^{Q209L}	[248]
Danio rerio	Mitfa$^{-/-}$, tp53$^{-/-}$	mitfa	GNAQ^{Q209L}, CYSTLR2^{L129Q}, YAP^{AA}, PLCB4^{D630Y}	[249]
Danio rerio	tp53$^{-/-}$, Mitfa$^{-/-}$; tp53$^{-/-}$	mitfa	GNAQ^{Q209L}, YAP$^{s127A;S381S}$, BRAF^{V600E}	[251]

flourish in the tissue from which they were derived [34]. One of the most important elements of generating translatable xenograft models, are using cell lines or tissue that resemble biology seen in UM patients. Most UM xenograft models have been generated with atypical $EIF1AX^{mut}$-cell line 92.1, and there is a clear lack of $BAP1^{mut}$-xenografts (Fig. 1C). Even though, these models have been useful to identify molecular pathways driving tumorigenesis (Fig. 2), current clinical care has excellent local tumor control but lack therapies for metastatic disease. Due to the high-risk of metastasis in $BAP1^{mut}$ UM, future xenograft studies should consider utilizing primary or/and metastatic high-risk cell lines ($SF3B1^{mut}$ and $BAP1^{mut}$-cells) instead of Gαq/11^{WT} or $EIF1AX^{mut}$-cells.

An interesting aspect is to increase our understanding of metastatic events is by investigating tumor-changes seen in the bloodstream of $BAP1^{mut}$-xenografts. Murine xenograft models have been used to identify circulating-tumor DNA *via* liquid-biopsies [253], illustrating these models could be utilized to study tumor-specific events in the bloodstream.

The majority of studies in our literature search are pharmacological studies and in general these pharmacological studies investigated primary driver mutation effects and inhibitors targeting the MEK-ERK pathway (Fig. 2–3, Table 1). Although driver mutations in UM (*Gαq, PLCB4, CYSLTR2*) are known to drive the MEK-ERK pathway, future studies should consider investigating the effects of secondary driver mutations (*EIF1AX, SF3B1 or BAP1*). Due to the difference in protein function and clinical outcome, we might gain most from studying effects seen due to secondary driver mutations. Unfortunately, thus far the majority of pharmacological studies are investigating tumor growth and lack data on metastasis. Nonetheless, several compounds inhibiting generic cancer pathways such as angiogenesis, NF-kB and CDKs were able to inhibit metastasis formation *in vivo* (Supplementary table 3). The anti-metastatic effect was seen in $BAP1^{WT}$-based xenograft models, which could prove difficulties towards clinical translatability as these compounds might act differently in $BAP1^{mut}$-UM (Fig. 4). The most noteworthy compounds evaluated *in vivo* were Withaferin A and GQ262. Withaferin A illustrated inhibitory effects in multiple pathways and provided complete remission in a subset of mice. GQ262 can be considered the most interesting candidate molecule for future studies and clinical trials. GQ262 targets mutant Gαq-proteins leading to complete remission in several mouse xenografts. Due to the high frequency of Gαq-mutations in UM [1], this compound has the potential to be applicable for the majority of UM patients regardless of secondary mutation.

The need for representable animal models for UM drug development are essential to evaluate treatment efficacy, however, after 40 years of UM animal models, the translatability has been unsatisfactory and unsuccessful. Only 1 published clinical trial utilized compounds tested in

have already shown this site is able to allow for tumor growth and metastasis [33,47–51]. Additionally, different inoculation sites can be used to improve liver metastasis formation for cell lines that lack metastatic capacity upon intraocular inoculation (*e.g.* splenic inoculation). However, engraftment can depend on inoculation site as some cell lines

an *in vivo* mouse model, yet synergistic effects seen in the mouse model were not reproduced in the trial (Table 6). This emphasizes the lack of translatable models, resulting in slow drug development strategies for metastatic UM. Therefore, we argue future xenograft models should take the following 4 points into consideration: 1) utilize *BAP1^{neg}*-UM cells, 2) when using primary UM cells use intraocular (preferably choroidal) inoculation, 3) if intraocular inoculation fails to show metastasis consider splenic inoculations to induce liver metastasis, 4) discover molecular mechanisms based on secondary driver mutations, especially by comparing *BAP1^{neg}*- UM cells to *BAP1^{pos}*-UM cells.

Transgenic UM models have so far failed to show a comparable course of disease, as these mouse models do not need secondary driver mutations to develop melanoma and fail to show liver metastasis. Recently, a UM mouse model utilizing *GNAQ^{mut}* and *BAP1*-deficent transgenes was described in preprint. This model illustrated potential liver metastasis and illustrated shared EMT-pathways between mouse and human UM [254]. Transgenic zebrafish models on the other hand do need secondary driver mutations to develop melanoma, yet the current models use loss of *p53* to induce melanoma. Both transgenic systems have been unsuccessful in inducing liver metastasis and struggle with tissue specificity, as they also develop cutaneous melanoma. To improve these models, information from single-cell experiments could elucidate unique factors of ocular pigmentation which can provide novel promotors to drive oncogenes restricted to the eyes. Additionally, combining ocular-specific expression with secondary mutations may provide models that resemble the natural behaviour of human UM more closely.

Financial support

CRediT authorship contribution statement

Quincy C.C. van den Bosch: Conceptualization, Investigation, Methodology, Visualization, Writing – original draft, Writing – review & editing. **Annelies de Klein:** Writing – review & editing. **Robert M. Verdijk:** Writing – review & editing. **Emine Kiliç:** Supervision, Funding acquisition, Writing – review & editing. **Erwin Brosens:** Conceptualization, Supervision, Funding acquisition, Writing – review & editing.

Declaration of Competing Interest

The authors declare that they have no known competing financial interests or personal relationships that could have appeared to influence the work reported in this paper.

Data availability

No data was used for the research described in the article.

Acknowledgments

Appendix A. Supplementary data

Supplementary data to this article can be found online at https://doi.org/10.1016/j.bbcan.2023.189055.

References

[1] M.J. Jager, et al., Uveal melanoma, Nat. Rev. Dis. Primers 6 (1) (2020) 24.

[2] W. Drabarek, et al., Multi-modality analysis improves survival prediction in enucleated uveal melanoma patients, Invest. Ophthalmol. Vis. Sci. 60 (10) (2019) 3595–3605.

[3] R.D. Carvajal, et al., Metastatic disease from uveal melanoma: treatment options and future prospects, British J 101 (1) (2017) 38–44.

[4] E.M. Damato, B.E. Damato, Detection and time to treatment of uveal melanoma in the United Kingdom: an evaluation of 2,384 patients, Ophthalmology 119 (8) (2012) 1582–1589.

[5] B. Damato, Does ocular treatment of uveal melanoma influence survival? Br. J. Cancer 103 (3) (2010) 285–290.

[6] M.J.C. Vader, et al., GNAQ and GNA11 mutations and downstream YAP activation in choroidal nevi, Br. J. Cancer 117 (6) (2017) 884–887.

[7] N.M. van Poppelen, et al., Genetic background of Iris melanomas and Iris melanocytic tumors of uncertain malignant potential, Ophthalmology 125 (6) (2018) 904–912.

[8] R.J. Nell, et al., Involvement of mutant and wild-type CYSLTR2 in the development and progression of uveal nevi and melanoma, BMC Cancer 21 (1) (2021) 164.

[9] M. Martin, et al., Exome sequencing identifies recurrent somatic mutations in EIF1AX and SF3B1 in uveal melanoma with disomy 3, Nat. Genet. 45 (8) (2013) 933–936.

[10] J.W. Harbour, et al., Recurrent mutations at codon 625 of the splicing factor SF3B1 in uveal melanoma, Nat. Genet. 45 (2) (2013) 133–135.

[11] J.W. Harbour, et al., Frequent mutation of BAP1 in metastasizing uveal melanomas, Science 330 (6009) (2010) 1410–1413.

[12] S. Yavuzyigitoglu, et al., Correlation of gene mutation status with copy number profile in uveal melanoma, Ophthalmology 124 (4) (2017) 573–575.

[13] C.L. Decatur, et al., Driver mutations in uveal melanoma: associations with gene expression profile and patient outcomes, JAMA Ophthalmol 134 (7) (2016) 728–733.

[14] K.N. Smit, et al., Uveal melanoma: towards a molecular understanding, Prog. Retin. Eye Res. 75 (2020), 100800.

[15] M.M. Golas, et al., Molecular architecture of the multiprotein splicing factor SF3b, Science 300 (5621) (2003) 980–984.

[16] A. Yoshimi, O. Abdel-Wahab, Splicing factor mutations in MDS RARS and MDS/MPN-RS-T, Int. J. Hematol. 105 (6) (2017) 720–731.

[17] C.P. Lapointe, et al., eIF5B and eIF1A reorient initiator tRNA to allow ribosomal subunit joining, Nature 607 (7917) (2022) 185–190.

[18] A. Marintchev, et al., Mapping the binding interface between human eukaryotic initiation factors 1A and 5B: a new interaction between old partners, Proc. Natl. Acad. Sci. U. S. A. 100 (4) (2003) 1535–1540.

[19] S. Yavuzyigitoglu, et al., Uveal melanomas with SF3B1 mutations: a distinct subclass associated with late-onset metastases, Ophthalmology 123 (5) (2016) 1118–1128.

[20] L. Khoja, et al., Meta-analysis in metastatic uveal melanoma to determine progression free and overall survival benchmarks: an international rare cancers initiative (IRCI) ocular melanoma study, Ann. Oncol. 30 (8) (2019) 1370–1380.

[21] E.S. Rantala, M. Hernberg, T.T. Kivelä, Overall survival after treatment for metastatic uveal melanoma: a systematic review and meta-analysis, Melanoma Res. 29 (6) (2019) 561–568.

[22] P. Nathan, et al., Overall survival benefit with Tebentafusp in metastatic uveal melanoma, N. Engl. J. Med. 385 (13) (2021) 1196–1206.

[23] A.H. Shain, et al., The genetic evolution of metastatic uveal melanoma, Nat. Genet. 51 (7) (2019) 1123–1130.

[24] W. Lin, et al., Intra- and intertumoral heterogeneity of liver metastases in a patient with uveal melanoma revealed by single-cell RNA sequencing, Cold Spring Harb. Mol. Case Stud. 7 (5) (2021).

[25] D.A. Rodriguez, et al., Multiregional genetic evolution of metastatic uveal melanoma, NPJ Genom. Med. 6 (1) (2021) 70.

[26] M.A. Durante, et al., Single-cell analysis reveals new evolutionary complexity in uveal melanoma, Nat. Commun. 11 (1) (2020) 496.

[27] M. Croce, et al., Targeted therapy of uveal melanoma: recent failures and new perspectives, Cancers (Basel) 11 (6) (2019).

[28] J.H. Nadeau, J. Auwerx, The virtuous cycle of human genetics and mouse models in drug discovery, Nat. Rev. Drug Discov. 18 (4) (2019) 255–272.

[29] C.R. Ireson, et al., The role of mouse tumour models in the discovery and development of anticancer drugs, Br. J. Cancer 121 (2) (2019) 101–108.

[30] E. Perez-Guijarro, et al., Genetically engineered mouse models of melanoma, Cancer 123 (2017) 2089–2103.

[31] J. Cao, M.J. Jager, Animal eye models for uveal melanoma, Ocul. Oncol. Pathol. 1 (3) (2015) 141–150.

[32] D. Süsskind, et al., Novel mouse model for primary uveal melanoma: a pilot study, Clin. Exp. Ophthalmol. 45 (2) (2017) 192–200.

[33] H. Yang, et al., In-vivo xenograft murine human uveal melanoma model develops hepatic micrometastases, Melanoma Res. 18 (2) (2008) 95–103.

[34] S. Ozaki, et al., Establishment and characterization of Orthotopic mouse models for human uveal melanoma hepatic colonization, Am. J. Pathol. 186 (1) (2016) 43–56.

[35] S. Heegaard, M. Spang-Thomsen, J.U. Prause, Establishment and characterization of human uveal malignant melanoma xenografts in nude mice, Melanoma Res. 13 (3) (2003) 247–251.

[36] K. Kageyama, et al., Establishment of an orthotopic patient-derived xenograft mouse model using uveal melanoma hepatic metastasis, J. Transl. Med. 15 (1) (2017).

[37] N. Amirouchene-Angelozzi, et al., Establishment of novel cell lines recapitulating the genetic landscape of uveal melanoma and preclinical validation of mTOR as a therapeutic target 8 (8) (2014) 1508–1520.

[38] M.J. Jager, et al., Uveal melanoma cell lines: where do they come from? (an American ophthalmological society Thesis), Trans. Am. Ophthalmol. Soc. 114 (2016) T5.

[39] F. Némati, et al., Establishment and characterization of a panel of human uveal melanoma xenografts derived from primary and/or metastatic tumors, Clin. Cancer Res. 16 (8) (2010) 2352–2362.

[40] F. Mouriaux, et al., Effects of long-term serial passaging on the characteristics and properties of cell lines derived from uveal melanoma primary tumors, Invest. Ophthalmol. Vis. Sci. 57 (13) (2016) 5288–5301.

[41] A. Groenewoud, G. Forn-Cuni, F.B. Engel, XePhIR: the zebrafish xenograft phenotype interactive repository, Database 2022 (2022) baac028.

[42] K.G. Griewank, et al., Genetic and molecular characterization of uveal melanoma cell lines, Pigment Cell Melanoma Res. 25 (2) (2012) 182–187.

[43] O.E. Uner, et al., Animal Models of Uveal Melanoma, 2022.

[44] D.M. Albert, M.D. Wagoner, K. Moazed, Heterotransplantation of human choroidal melanoma into the athymic 'nude' mouse, Invest. Ophthalmol. Vis. Sci. 19 (5) (1980) 555–559.

[45] T. Sugase, et al., Development and optimization of orthotopic liver metastasis xenograft mouse models in uveal melanoma, J. Transl. Med. 18 (1) (2020).

[46] P.T. Logan, et al., Single-cell tumor dormancy model of uveal melanoma, Clin. Exp. Metastasis 25 (5) (2008) 509–516.

[47] A.C. Repp, et al., Role of Fas ligand in uveal melanoma-induced liver damage, Graefes Arch. Clin. Exp. Ophthalmol. 239 (10) (2001) 752–758.

[48] D. Ma, J.Y. Niederkorn, Role of epidermal growth factor receptor in the metastasis of intraocular melanomas, Invest. Ophthalmol. Vis. Sci. 39 (7) (1998) 1067–1075.

[49] H. Yang, M.J. Jager, H.E. Grossniklaus, Bevacizumab suppression of establishment of micrometastases in experimental ocular melanoma, Invest. Ophthalmol. Vis. Sci. 51 (6) (2010) 2835–2842.

[50] Z. Liang, et al., Development of a unique small molecule modulator of cxcr4, PLoS One (2012) 7(4).

[51] R. Ramos, et al., Orthotopic murine xenograft model of uveal melanoma with spontaneous liver metastasis, Melanoma Res. 33 (1) (2023) 1–11.

[52] C.D. Van Raamsdonk, et al., Frequent somatic mutations of GNAQ in uveal melanoma and blue naevi, Nature 457 (7229) (2009) 599–602.

[53] C.D. Van Raamsdonk, et al., Mutations in GNA11 in uveal melanoma, New Engl. J. Med. 363 (23) (2010) 2191–2199.

[54] A.R. Moore, et al., Recurrent activating mutations of G-protein-coupled receptor CYSLTR2 in uveal melanoma, Nat. Genet. 48 (6) (2016) 675–680.

[55] P. Johansson, et al., Deep sequencing of uveal melanoma identifies a recurrent mutation in PLCB4, Oncotarget 7 (4) (2016) 4624–4631.

[56] J.S. Paradis, et al., Synthetic lethal screens reveal cotargeting FAK and MEK as a multimodal precision therapy for GNAQ-driven uveal melanoma, Clin. Cancer Res. 27 (11) (2021) 3190–3200.

[57] R. Vivet-Noguer, et al., Emerging therapeutic opportunities based on current knowledge of uveal melanoma biology, Cancers 11 (7) (2019) 1019.

[58] J. Bauer, et al., Oncogenic GNAQ mutations are not correlated with disease-free survival in uveal melanoma, Br. J. Cancer 101 (5) (2009) 813–815.

[59] F. Piaggio, et al., In uveal melanoma Gα-protein GNA11 mutations convey a shorter disease-specific survival and are more strongly associated with loss of BAP1 and chromosomal alterations than Gα-protein GNAQ mutations, Eur. J. Cancer 170 (2022) 27–41.

[60] M. Gabay, et al., Ric-8 proteins are molecular chaperones that direct nascent G protein alpha subunit membrane association, Sci. Signal. 4 (200) (2011) ra79.

[61] B.R. Patel, G.G. Tall, Ric-8A gene deletion or phorbol ester suppresses tumorigenesis in a mouse model of GNAQQ209L-driven melanoma, Oncogenesis 5 (6) (2016).

[62] F.X. Yu, et al., Regulation of the hippo-YAP pathway by G-protein-coupled receptor signaling, Cell 150 (4) (2012) 780–791.

[63] S. Piccolo, S. Dupont, M. Cordenonsi, The biology of YAP/TAZ: hippo signaling and beyond, Physiol. Rev. 94 (4) (2014) 1287–1312.

[64] F.X. Yu, et al., Mutant Gq/11 promote uveal melanoma tumorigenesis by activating YAP, Cancer Cell 25 (6) (2014) 822–830.

[65] Y. Sun, et al., Pharmacological blockade of TEAD–YAP reveals its therapeutic limitation in cancer cells, Nat. Commun. 13 (1) (2022).

[66] X. Feng, et al., Hippo-independent activation of YAP by the GNAQ uveal melanoma oncogene through a trio-regulated rho GTPase signaling circuitry, Cancer Cell 25 (6) (2014) 831–845.

[67] N. Mosaddeghzadeh, M.R. Ahmadian, The RHO family GTPases: mechanisms of regulation and signaling, Cells 10 (7) (2021).

[68] J.H. Yoo, et al., ARF6 is an actionable node that orchestrates oncogenic GNAQ signaling in uveal melanoma, Cancer Cell 29 (6) (2016) 889–904.

[69] P.S. Steeg, et al., Evidence for a novel gene associated with low tumor metastatic potential, J. Natl. Cancer Inst. 80 (3) (1988) 200–204.

[70] S. Bakalian, et al., Expression of nm23-H1 in uveal melanoma, Melanoma Res. 17 (5) (2007) 284–290.

[71] D. Ma, et al., Association between NM23-H1 gene expression and metastasis of human uveal melanoma in an animal model, Invest. Ophthalmol. Vis. Sci. 37 (11) (1996) 2293–2301.

[72] B. Kim, K.-J. Lee, Activation of Nm23-H1 to suppress breast cancer metastasis via redox regulation, Exp. Mol. Med. 53 (3) (2021) 346–357.

[73] W.G. Jiang, M.B. Hallett, M.C. Puntis, Hepatocyte growth factor/scatter factor, liver regeneration and cancer metastasis, Br. J. Surg. 80 (11) (1993) 1368–1373.

[74] J. Fu, et al., HGF/c-MET pathway in cancer: from molecular characterization to clinical evidence, Oncogene 40 (28) (2021) 4625–4651.

[75] F.P. Gardner, et al., C-MET expression in primary and liver metastases in uveal melanoma, Melanoma Res. 24 (6) (2014) 617–620.

[76] R. Gangemi, et al., ADAM10 correlates with uveal melanoma metastasis and promotes in vitro invasion, Pigment Cell Melanoma Res. 27 (6) (2014) 1138–1148.

[77] G. Barisione, et al., Potential role of soluble c-met as a new candidate biomarker of metastatic uveal melanoma, JAMA Ophthalmol 133 (9) (2015) 1013–1021.

[78] R. Tanaka, et al., The role of HGF/MET signaling in metastatic uveal melanoma, Cancers (Basel) 13 (21) (2021).

[79] G. Yu, et al., Hepatic stellate cells secreted hepatocyte growth factor contributes to the chemoresistance of hepatocellular carcinoma, PLoS One 8 (9) (2013), e73312.

[80] C. Yin, et al., Hepatic stellate cells in liver development, regeneration, and cancer, J. Clin. Invest. 123 (5) (2013) 1902–1910.

[81] L. Piquet, et al., Synergic interactions between hepatic stellate cells and uveal melanoma in metastatic growth, Cancers 11 (8) (2019).

[82] G. Ambrosini, et al., Uveal melanoma exosomes induce a Prometastatic microenvironment through macrophage migration inhibitory factor, Mol. Cancer Res. 20 (4) (2022) 661–669.

[83] D.C. Branisteanu, et al., Uveal melanoma diagnosis and current treatment options (review), Exp. Ther. Med. 22 (6) (2021) 1428.

[84] E. Kilic, et al., Clinical and cytogenetic analyses in uveal melanoma, Invest. Ophthalmol. Vis. Sci. 47 (9) (2006) 3703–3707.

[85] Z. Fan, et al., SLC25A38 as a novel biomarker for metastasis and clinical outcome in uveal melanoma, Cell Death Dis. 13 (4) (2022).

[86] R. Gangemi, et al., Mda-9/syntenin is expressed in uveal melanoma and correlates with metastatic progression, PLoS One (2012) 7(1).

[87] P. Milan-Rois, et al., The role of LncRNAs in uveal melanoma, Cancers (Basel) 13 (16) (2021).

[88] S.J. Liu, et al., Long noncoding RNAs in cancer metastasis, Nat. Rev. Cancer 21 (7) (2021) 446–460.

[89] P. Li, et al., ZNNT1 long noncoding RNA induces autophagy to inhibit tumorigenesis of uveal melanoma by regulating key autophagy gene expression, Autophagy 16 (7) (2020) 1186–1199.

[90] Y. Qi, et al., Knockdown of long non-coding rna loc100132707 inhibits the migration of uveal melanoma cells via silencing jak2, OncoTargets Ther. 13 (2020) 12955–12964.

[91] S.J. Thomas, et al., The role of JAK/STAT signalling in the pathogenesis, prognosis and treatment of solid tumours, Br. J. Cancer 113 (3) (2015) 365–371.

[92] D. Peng, et al., MiR-142-3p suppresses uveal melanoma by targeting CDC25C, TGFβR1, GNAQ, WASL, and RAC1, Cancer Manag. Res. 11 (2019) 4729–4742.

[93] S. Schubbert, K. Shannon, G. Bollag, Hyperactive Ras in developmental disorders and cancer, Nat. Rev. Cancer 7 (4) (2007) 295–308.

[94] U. Keilholz, et al., ESMO consensus conference recommendations on the management of metastatic melanoma: under the auspices of the ESMO guidelines committee, Ann. Oncol. 31 (11) (2020) 1435–1448.

[95] T. Steeb, et al., How to MEK the best of uveal melanoma: a systematic review on the efficacy and safety of MEK inhibitors in metastatic or unresectable uveal melanoma, Eur. J. Cancer 103 (2018) 41–51.

[96] H. Cheng, et al., Paracrine effect of NRG1 and HGF drives resistance to MEK inhibitors in metastatic uveal melanoma, Cancer Res. 75 (13) (2015) 2737–2748.

[97] M. Bhargava, et al., Scatter factor and hepatocyte growth factor: activities, properties, and mechanism, Cell Growth Differ. 3 (1) (1992) 11–20.

[98] X. Feng, et al., A platform of synthetic lethal gene interaction networks reveals that the GNAQ uveal melanoma oncogene controls the hippo pathway through FAK, Cancer Cell 35 (3) (2019) 457–472.e5.

[99] X. Chen, et al., Combined PKC and MEK inhibition in uveal melanoma with GNAQ and GNA11 mutations, Oncogene 33 (39) (2014) 4724–4734.

[100] A.A. Amaro, et al., Cerivastatin synergizes with Trametinib and enhances its efficacy in the therapy of uveal melanoma, Cancers (Basel) 15 (3) (2023).

[101] N. Babchia, et al., The PI3K/Akt and mTOR/P70S6K signaling pathways in human uveal melanoma cells: interaction with B-Raf/ERK, Invest. Ophthalmol. Vis. Sci. 51 (1) (2010) 421–429.

[102] G. Ambrosini, et al., Inhibition of mutant GNAQ signaling in uveal melanoma induces AMPK-dependent autophagic cell death, Mol. Cancer Ther. 12 (5) (2013) 768–776.

[103] G. Carita, et al., Dual inhibition of protein kinase C and p53-MDM2 or PKC and mTORC1 are novel efficient therapeutic approaches for uveal melanoma, Oncotarget 7 (23) (2016) 33542–33556.

[104] A.K. Samadi, et al., Natural withanolide withaferin a induces apoptosis in uveal melanoma cells by suppression of Akt and c-MET activation, Tumor Biol 33 (4) (2012) 1179–1189.

[105] D.P. Mangiameli, et al., Combination therapy targeting the tumor microenvironment is effective in a model of human ocular melanoma, J. Transl. Med. 5 (2007).

[106] E. Musi, et al., The phosphoinositide 3-kinase a selective inhibitor BYL719 enhances the effect of the protein kinase C inhibitor AEB071 in GNAQ/GNA11-mutant uveal melanoma cells, Mol. Cancer Ther. 13 (5) (2014) 1044–1053.

[107] K.N. Smit, et al., Genome-wide aberrant methylation in primary metastatic UM and their matched metastases, Sci. Rep. 12 (1) (2022) 42.

[108] F. Lyko, The DNA methyltransferase family: a versatile toolkit for epigenetic regulation, Nat. Rev. Genet. 19 (2) (2018) 81–92.

[109] X. Gu, et al., Epigenetic drug library screening reveals targeting DOT1L abrogates NAD+ synthesis by reprogramming H3K79 methylation in uveal melanoma, J. Pharmaceut Analy 13 (1) (2023) 24–38.

[110] J. Gonçalves, et al., Decitabine limits escape from MEK inhibition in uveal melanoma, Pigm Cell Melanoma Res 33 (3) (2020) 507–514.

[111] D. Hanahan, R.A. Weinberg, Hallmarks of cancer: the next generation, Cell 144 (5) (2011) 646–674.

[112] I. Bose, B. Ghosh, The p53-MDM2 network: from oscillations to apoptosis, J. Biosci. 32 (5) (2007) 991–997.

[113] M. Redza-Dutordoir, D.A. Averill-Bates, Activation of apoptosis signalling pathways by reactive oxygen species, Biochim. Biophys. Acta 1863 (12) (2016) 2977–2992.

[114] R.K. Blackman, et al., Mitochondrial electron transport is the cellular target of the oncology drug elesclomol, PLoS One 7 (1) (2012), e29798.

[115] Y. Li, et al., Copper ionophore elesclomol selectively targets GNAQ/11-mutant uveal melanoma, Oncogene 41 (27) (2022) 3539–3553.

[116] J.M. Mulcahy Levy, A. Thorburn, Autophagy in cancer: moving from understanding mechanism to improving therapy responses in patients, Cell Death Differ. 27 (3) (2020) 843–857.

[117] A. Truong, et al., Chloroquine sensitizes GNAQ/11-mutated melanoma to MEK1/2 inhibition, Clin. Cancer Res. 26 (23) (2020) 6374–6386.

[118] X. Fei, et al., Proteomics analysis: inhibiting the expression of P62 protein by chloroquine combined with dacarbazine can reduce the malignant progression of uveal melanoma, BMC Cancer 22 (1) (2022).

[119] L. de Koning, et al., Parp inhibition increases the response to chemotherapy in uveal melanoma, Cancers 11 (6) (2019).

[120] H. Kang, et al., (−)-4-O-(4-O-β-D-glucopyranosylcaffeoyl) quinic acid exerts anti-tumour effects against uveal melanoma through PI3K/AKT pathway, Cutan. Ocul. Toxicol. 40 (2) (2021) 119–124.

[121] A. Latorre, et al., Albumin-based nanostructures for uveal melanoma treatment, Nanomedicine (2021) 35.

[122] S. Kaochar, et al., ICG-001 exerts potent anticancer activity against uveal melanoma cells, Invest. Ophthalmol. Vis. Sci. 59 (1) (2018) 132–143.

[123] N. Amirouchene-Angelozzi, et al., The mTOR inhibitor Everolimus synergizes with the PI3K inhibitor GDC0941 to enhance anti-tumor efficacy in uveal melanoma, Oncotarget 7 (17) (2016) 23633–23646.

[124] O. Surriga, et al., Crizotinib, a c-met inhibitor, prevents metastasis in a metastatic uveal melanoma model, Mol. Cancer Ther. 12 (12) (2013) 2817–2826.

[125] S.C. Lee, et al., Cordycepin (3′-deoxyadenosine) suppresses heat shock protein 90 function and targets tumor growth in an adenosine deaminase-dependent manner, Cancers 14 (13) (2022).

[126] D. Wootten, et al., Mechanisms of signalling and biased agonism in G protein-coupled receptors, Nat. Rev. Mol. Cell Biol. 19 (10) (2018) 638–653.

[127] H. Li, H. Alizadeh, J.Y. Niederkorn, Differential expression of chemokine receptors on uveal melanoma cells and their metastases, Invest. Ophthalmol. Vis. Sci. 49 (2) (2008) 636–643.

[128] H. Li, et al., Inhibition of chemokine receptor expression on uveal melanomas by CXCR4 siRNA and its effect on uveal melanoma liver metastases, Invest. Ophthalmol. Vis. Sci. 50 (12) (2009) 5522–5528.

[129] S. Scala, et al., CXC chemokine receptor 4 is expressed in uveal malignant melanoma and correlates with the epithelioid-mixed cell type, Cancer Immunol. Immunother. 56 (10) (2007) 1589–1595.

[130] T. van den Bosch, et al., Chemokine receptor CCR7 expression predicts poor outcome in uveal melanoma and relates to liver metastasis whereas expression of CXCR4 is not of clinical relevance, Invest. Ophthalmol. Vis. Sci. 54 (12) (2013) 7354–7361.

[131] H. Yang, et al., Non-invasive detection and complementary diagnostic of liver metastases via chemokine receptor 4 imaging, Cancer Gene Ther 29 (12) (2022) 1827–1839.

[132] S. Tan, et al., Chemokine receptor 4 targeted protein MRI contrast agent for early detection of liver metastases, Sci. Adv. 6 (6) (2020) eaav7504.

[133] D.M. Kemp, et al., Ladarixin, a dual CXCR1/2 inhibitor, attenuates experimental melanomas harboring different molecular defects by affecting malignant cells and tumor microenvironment, Oncotarget 8 (9) (2017) 14428–14442.

[134] A. Zhu, et al., Dipyrimidine amines: a novel class of chemokine receptor type 4 antagonists with high specificity, J. Med. Chem. 53 (24) (2010) 8556–8568.

[135] Z. Abdel-Malek, et al., The melanocortin-1 receptor is a key regulator of human cutaneous pigmentation, Pigment Cell Res. 13 (Suppl. 8) (2000) 156–162.

[136] M.N. Lopez, et al., Melanocortin 1 receptor is expressed by uveal malignant melanoma and can be considered a new target for diagnosis and immunotherapy, Invest. Ophthalmol. Vis. Sci. 48 (3) (2007) 1219–1227.

[137] N.K. Tafreshi, et al., Melanocortin 1 receptor–targeted a-particle therapy for metastatic uveal melanoma, J. Nucl. Med. 60 (8) (2019) 1124–1133.

[138] M.D. Onken, et al., Targeting primary and metastatic uveal melanoma with a G protein inhibitor, J. Biol. Chem. 296 (2021).

[139] Y. Ge, et al., Design, synthesis, and evaluation of small molecule Gαq/11 protein inhibitors for the treatment of uveal melanoma, J. Med. Chem. 64 (6) (2021) 3131–3152.

[140] M.D. Onken, et al., Oncogenic Gq/11 signaling acutely drives and chronically sustains metabolic reprogramming in uveal melanoma, J. Biol. Chem. 298 (1) (2022).

[141] D. Lapadula, et al., IGF1R Inhibition Enhances the Therapeutic Effects of Gq/11 Inhibition in Metastatic Uveal Melanoma Progression, Molecular Cancer, 2023.

[142] C. Chattopadhyay, et al., Targeting IRS-1/2 in uveal melanoma inhibits in vitro cell growth, survival and migration, and in vivo tumor growth, Cancers 14 (24) (2022).

[143] A. Girnita, et al., The insulin-like growth factor-I receptor inhibitor picropodophyllin causes tumor regression and attenuates mechanisms involved in invasion of uveal melanoma cells, Acta Ophthalmol. 86 (THESIS 4) (2008) 26–34.

[144] S. Mohan, D.J. Baylink, IGF-binding proteins are multifunctional and act via IGF-dependent and -independent mechanisms, J. Endocrinol. 175 (1) (2002) 19–31.

[145] Y. Ge, et al., Discovery of small molecule Gαq/11 protein inhibitors against uveal melanoma, Acta Pharm. Sin. B 12 (8) (2022) 3326–3340.

[146] S.H. Kaufmann, W.C. Earnshaw, Induction of apoptosis by cancer chemotherapy, Exp. Cell Res. 256 (1) (2000) 42–49.

[147] K. Glinkina, et al., Preclinical evaluation of Trabectedin in combination with targeted inhibitors for treatment of metastatic uveal melanoma, Invest. Ophthalmol. Vis. Sci. 63 (13) (2022).

[148] Q. Zhu, et al., Cepharanthine exerts antitumor activity on choroidal melanoma by reactive oxygen species production and c-Jun N-terminal kinase activation, Oncol. Lett. 13 (5) (2017) 3760–3766.

[149] N. Mukherjee, et al., Expression differences in BCL2 family members between uveal and cutaneous melanomas account for varying sensitivity to BH3 mimetics, J. Invest. Dermatol. 142 (7) (2022) 1912–1922.e7.

[150] U. Asghar, et al., The history and future of targeting cyclin-dependent kinases in cancer therapy, Nat. Rev. Drug Discov. 14 (2) (2015) 130–146.

[151] H. Zhao, et al., SKP2 targeted inhibition suppresses human uveal melanoma progression by blocking ubiquitylation of p27, OncoTargets Ther. 12 (2019) 4297–4308.

[152] J.L.F. Teh, et al., Metabolic adaptations to MEK and CDK4/6 cotargeting in uveal melanoma, Mol. Cancer Ther. 19 (8) (2020) 1719–1726.

[153] M. Ohara, et al., Dual targeting of cdk4/6 and cmet in metastatic uveal melanoma, Cancers 13 (5) (2021) 1–19.

[154] J. Zhang, et al., Transcriptional inhibition by CDK7/9 inhibitor SNS-032 abrogates oncogene addiction and reduces liver metastasis in uveal melanoma, Mol. Cancer 18 (1) (2019).

[155] L. Dong, et al., Arylsulfonamide 64B inhibits hypoxia/ HIF-induced expression of c-met and CXCR4 and reduces primary tumor growth and metastasis of uveal melanoma, Clin. Cancer Res. 25 (7) (2019) 2206–2218.

[156] S. Kaluz, et al., Targeting HIF-activated collagen prolyl 4-hydroxylase expression disrupts collagen deposition and blocks primary and metastatic uveal melanoma growth, Oncogene 40 (33) (2021) 5182–5191.

[157] P.S. Steeg, Tumor metastasis: mechanistic insights and clinical challenges, Nat. Med. 12 (8) (2006) 895–904.

[158] K. Taniguchi, M. Karin, NF-κB, inflammation, immunity and cancer: coming of age, Nat. Rev. Immunol. 18 (5) (2018) 309–324.

[159] R. Dror, et al., Characterizing the involvement of the nuclear factor-kappa B (NF kappa B) transcription factor in uveal melanoma, Invest. Ophthalmol. Vis. Sci. 51 (4) (2010) 1811–1816.

[160] J. Zhou, et al., The antihelminthic drug niclosamide effectively inhibits the malignant phenotypes of uveal melanoma in vitro and in vivo, Theranostics 7 (6) (2017) 1447–1462.

[161] E. Musi, et al., Tris DBA palladium is an orally available inhibitor of GNAQ mutant uveal melanoma in vivo, Oncotarget 10 (43) (2019) 4424–4436.

[162] Y. Jin, et al., Neddylation blockade diminishes hepatic metastasis by dampening cancer stem-like cells and angiogenesis in uveal melanoma, Clin. Cancer Res. 24 (15) (2018) 3741–3754.

[163] J. Zhou, et al., Salinomycin effectively eliminates cancer stem-like cells and obviates hepatic metastasis in uveal melanoma, Mol. Cancer 18 (1) (2019).

[164] B. Jin, et al., Verification of EZH2 as a druggable target in metastatic uveal melanoma, Mol. Cancer 19 (1) (2020).

[165] S.H. Chang, et al., Prognostic biomarkers in uveal melanoma: evidence for a stem cell-like phenotype associated with metastasis, Melanoma Res. 18 (3) (2008) 191–200.

[166] K.A. Matatall, et al., BAP1 deficiency causes loss of melanocytic cell identity in uveal melanoma, BMC Cancer 13 (2013).

[167] S. Landreville, et al., Histone deacetylase inhibitors induce growth arrest and differentiation in uveal melanoma, Clin. Cancer Res. 18 (2) (2012) 408–416.

[168] M.A. Glozak, E. Seto, Histone deacetylases and cancer, Oncogene 26 (37) (2007) 5420–5432.

[169] J.N. Kuznetsoff, et al., Dual screen for efficacy and toxicity identifies HDAC inhibitor with distinctive activity spectrum for BAP1-mutant uveal melanoma, Mol. Cancer Res. 19 (2) (2021) 215–222.

[170] Y. Wang, et al., In vitro and in vivo anti-uveal melanoma activity of JSL-1, a novel HDAC inhibitor, Cancer Lett. 400 (2017) 47–60.

[171] J.J. Sacco, et al., Loss of the deubiquitylase BAP1 alters class I histone deacetylase expression and sensitivity of mesothelioma cells to HDAC inhibitors, Oncotarget 6 (15) (2015) 13757–13771.

[172] T. Yamano, et al., Splicing modulator FR901464 is a potential agent for colorectal cancer in combination therapy, Oncotarget 10 (3) (2019) 352–367.

[173] T. Fujisawa, P. Filippakopoulos, Functions of bromodomain-containing proteins and their roles in homeostasis and cancer, Nat. Rev. Mol. Cell Biol. 18 (4) (2017) 246–262.

[174] A. Stathis, F. Bertoni, BET proteins as targets for anticancer treatment, Cancer Discov. 8 (1) (2018) 24–36.

[175] T. van den Bosch, et al., Higher percentage of FISH-determined monosomy 3 and 8q amplification in uveal melanoma cells relate to poor patient prognosis, Invest. Ophthalmol. Vis. Sci. 53 (6) (2012) 2668–2674.

[176] P. Filippakopoulos, et al., Selective inhibition of BET bromodomains, Nature 468 (7327) (2010) 1067–1073.

[177] G. Ambrosini, et al., BRD4-targeted therapy induces Myc-independent cytotoxicity in Gnaq/11-mutatant uveal melanoma cells, Oncotarget 6 (32) (2015) 33397–33409.

[178] G.M. Zhang, et al., Reciprocal positive regulation between BRD4 and YAP in GNAQ-mutant uveal melanoma cells confers sensitivity to BET inhibitors, Pharmacol. Res. 184 (2022).

[179] C.Y. Fong, et al., BET inhibitor resistance emerges from leukaemia stem cells, Nature 525 (7570) (2015) 538–542.

[180] P. Rathert, et al., Transcriptional plasticity promotes primary and acquired resistance to BET inhibition, Nature 525 (7570) (2015) 543–547.

[181] G. Ambrosini, et al., Inhibition of NF-κB-dependent signaling enhances sensitivity and overcomes resistance to bet inhibition in uveal melanoma, Cancer Res. 79 (9) (2019) 2415–2425.

[182] V. Chua, et al., Stromal fibroblast growth factor 2 reduces the efficacy of bromodomain inhibitors in uveal melanoma, EMBO Mol. Med. 11 (2) (2019).

[183] T.H. Van Essen, et al., Upregulation of HLA expression in primary uveal melanoma by infiltrating leukocytes, PLoS One 11 (10) (2016).

[184] J.Y. Niederkorn, et al., Effect of anti-ganglioside antibodies on the metastatic spread of intraocular melanomas in a nude mouse model of human uveal melanoma, Curr. Eye Res. 12 (4) (1993) 347–358.

[185] R. Crépin, D. Gentien, A. Duché, Nanobodies against Surface Biomarkers Enable the Analysis of Tumor Genetic Heterogeneity in Uveal Melanoma Patient-Derived Xenografts, Pigment Cell, 2017.

[186] R. Zhang, et al., Inhibition of CD146 lessens uveal melanoma progression through reducing angiogenesis and vasculogenic mimicry, Cell. Oncol. 45 (4) (2022) 557–572.

[187] A.C. Filley, M. Dey, Immune system, friend or foe of oncolytic Virotherapy? Front. Oncol. 7 (2017) 106.

[188] R.P.M. Sutmuller, et al., Adoptive T cell immunotherapy of human uveal melanoma targeting gp100, J. Immunol. 165 (12) (2000) 7308–7315.

[189] D. Martinez-Perez, et al., Gp-100 as a novel therapeutic target in uveal melanoma, Cancers (Basel) 13 (23) (2021).

[190] R.C. Kines, et al., An infrared dye-conjugated virus-like particle for the treatment of primary uveal melanoma, Mol. Cancer Ther. 17 (2) (2018) 565–574.

[191] T. Roe, et al., Integration of murine leukemia virus DNA depends on mitosis, EMBO J. 12 (5) (1993) 2099–2108.

[192] H. Voropaev, et al., Infectious knockdown of CREB and HIF-1 for the treatment of metastatic uveal melanoma, Cancers 11 (8) (2019).

[193] S. Liu, et al., Macrophage polarization contributes to the efficacy of an oncolytic HSV-1 targeting human uveal melanoma in a murine xenograft model, Exp. Eye Res. 202 (2021), 108285.

[194] D. Ma, et al., Relationship between natural killer cell susceptibility and metastasis of human uveal melanoma cells in a murine model, Invest. Ophthalmol. Vis. Sci. 36 (2) (1995) 435–441.

[195] S. Berghmans, et al., Making waves in cancer research: new models in the zebrafish, Biotechniques 39 (2) (2005) 227–237.

[196] K. Liu, et al., Expanding the CRISPR toolbox in zebrafish for studying development and disease, Front. Cell Dev. Biol. 7 (2019) 13.

[197] K. Howe, et al., The zebrafish reference genome sequence and its relationship to the human genome, Nature 496 (7446) (2013) 498–503.

[198] M. Fazio, et al., Zebrafish patient avatars in cancer biology and precision cancer therapy, Nat. Rev. Cancer 20 (5) (2020) 263–273.

[199] S.H. Lam, et al., Development and maturation of the immune system in zebrafish, Danio rerio: a gene expression profiling, in situ hybridization and immunological study, Dev. Comp. Immunol. 28 (1) (2004) 9–28.

[200] C.B. Kimmel, et al., Stages of embryonic development of the zebrafish, Dev. Dyn. 203 (3) (1995) 253–310.

[201] G. Fornabaio, et al., Angiotropism and extravascular migratory metastasis in cutaneous and uveal melanoma progression in a zebrafish model, Sci. Rep. 8 (1) (2018) 10448.

[202] W. van der Ent, et al., Modeling of human uveal melanoma in zebrafish xenograft embryos, Invest. Ophthalmol. Vis. Sci. 55 (10) (2014) 6612–6622.

[203] M.G. Haney, L.H. Moore, J.S. Blackburn, Drug screening of primary patient derived tumor xenografts in zebrafish, J. Vis. Exp. 158 (2020).

[204] A.J. Rennekamp, R.T. Peterson, 15 years of zebrafish chemical screening, Curr. Opin. Chem. Biol. 24 (2015) 58–70.

[205] W. Van Der Ent, et al., Embryonic zebrafish: different phenotypes after injection of human uveal melanoma cells, Ocul. Oncol. Pathol. 1 (3) (2015) 170–181.

[206] H. Sundaramurthi, et al., Uveal melanoma cell line proliferation is inhibited by Ricolinostat, a histone deacetylase inhibitor, Cancers 14 (3) (2022).

[207] K. Slater, et al., High cysteinyl leukotriene receptor 1 expression correlates with poor survival of uveal melanoma patients and cognate antagonist drugs modulate the growth, cancer secretome, and metabolism of uveal melanoma cells, Cancers 12 (10) (2020) 1–27.

[208] Y. Ding, et al., Dose-Dependent Carbon-dot-Induced ROS Promote Uveal Melanoma Cell Tumorigenicity Via Activation of mTOR Signaling and Glutamine Metabolism, Advanced …, 2021.

[209] J. Yin, et al., Zebrafish patient-derived xenograft model as a preclinical platform for uveal melanoma drug discovery, Pharmaceuticals 16 (4) (2023).

[210] A. Groenewoud, et al., Patient-derived zebrafish xenografts of uveal melanoma reveal ferroptosis as a drug target, Cell Death Dis. 9 (1) (2023) 183.

[211] L. Yu, et al., Co-occurrence of BAP1 and SF3B1 mutations in uveal melanoma induces cellular senescence, Mol. Oncol. 16 (3) (2022) 607–629.

[212] S. Bauer, et al., A phase Ib trial of combined PKC and MEK inhibition with sotrastaurin and binimetinib in patients with metastatic uveal melanoma, Front. Oncol. 12 (2022), 975642.

[213] A. Richmond, Y. Su, Mouse xenograft models vs GEM models for human cancer therapeutics, Dis. Model. Mech. 1 (2–3) (2008) 78–82.

[214] O.J. Becher, E.C. Holland, Genetically engineered models have advantages over xenografts for preclinical studies, Cancer Res. 66 (7) (2006) 3355–3358 (discussion 3358–9).

[215] M. Bradl, et al., Malignant melanoma in transgenic mice, Proc. Natl. Acad. Sci. U. S. A. 88 (1) (1991) 164–168.

[216] A. Klein-Szanto, et al., Melanosis and associated tumors in transgenic mice, Proc. Natl. Acad. Sci. U. S. A. 88 (1) (1991) 169–173.

[217] R. Anand, et al., Characterization of intraocular tumors arising in transgenic mice, Invest. Ophthalmol. Vis. Sci. 35 (9) (1994) 3533–3539.

[218] G. De la Houssaye, et al., ETS-1 and ETS-2 are upregulated in a transgenic mouse model of pigmented ocular neoplasm, Mol. Vis. 14 (2008) 1912–1928.

[219] D. Penna, A. Schmidt, F. Beermann, Tumors of the retinal pigment epithelium metastasize to inguinal lymph nodes and spleen in tyrosinase-related protein 1/ SV40 T antigen transgenic mice, Oncogene 17 (20) (1998) 2601–2607.

[220] N.A. Syed, et al., Transgenic mice with pigmented intraocular tumors: tissue of origin and treatment, Invest. Ophthalmol. Vis. Sci. 39 (13) (1998) 2800–2805.

[221] D.M. Albert, et al., Effectiveness of 1α-hydroxyvitamin D2 in inhibiting tumor growth in a murine transgenic pigmented ocular tumor model, Arch. Ophthalmol. 122 (9) (2004) 1365–1369.

[222] S. Wang, et al., Suppression of thrombospondin-1 expression during uveal melanoma progression and its potential therapeutic utility, Arch. Ophthalmol. 130 (3) (2012) 336–341.

[223] M.D. Onken, et al., Functional gene expression analysis uncovers phenotypic switch in aggressive uveal melanomas, Cancer Res. 66 (9) (2006) 4602–4609.

[224] M. Broome Powell, et al., Hyperpigmentation and melanocytic hyperplasia in transgenic mice expressing the human T24 ha-ras gene regulated by a mouse tyrosinase promoter, Mol. Carcinog. 12 (2) (1995) 82–90.

[225] R. Sutton, et al., Tyr-TGFα transgenic mice develop ocular melanocytic lesions, Melanoma Res. 12 (5) (2002) 435–439.

[226] T.R. Kramer, et al., Pigmented uveal tumours in a transgenic mouse model, Br. J. Ophthalmol. 82 (8) (1998) 953–960.

[227] W.H. Tolleson, et al., Spontaneous uveal amelanotic melanoma in transgenic Tyr-RAS Ink4a/Arf−/− mice, Arch. Ophthalmol. 123 (8) (2005) 1088–1094.

[228] A. Tanaka, et al., Whole recombinant yeast vaccine induces antitumor immunity and improves survival in a genetically engineered mouse model of melanoma, Gene Ther 18 (8) (2011) 827–834.

[229] J. Zhu, et al., Resistance to cancer immunotherapy mediated by apoptosis of tumor-infiltrating lymphocytes, Nat. Commun. 8 (1) (2017).

[230] S. Schiffner, et al., Tg(Grm1) transgenic mice: a murine model that mimics spontaneous uveal melanoma in humans? Exp. Eye Res. 127 (2014) 59–68.

[231] H. Li, et al., YAP/TAZ activation drives uveal melanoma initiation and progression, Cell Rep. 29 (10) (2019) 3200–3211.e4.

[232] M.K. Leonard, et al., Comprehensive molecular profiling of UV-induced metastatic melanoma in Nme1/Nme2-deficient mice reveals novel markers of survival in human patients, Oncogene 40 (45) (2021) 6329–6342.

[233] E. Dabbeche-Bouricha, et al., Rapid dissemination of RET-transgene-driven melanoma in the presence of non-obese diabetic alleles: critical roles of Dectin-1 and nitric-oxide synthase type 2, OncoImmunology 5 (5) (2016).

[234] Y.K. Pin, et al., Lymphadenectomy promotes tumor growth and cancer cell dissemination in the spontaneous RET mouse model of human uveal melanoma, Oncotarget 6 (42) (2015) 44806–44818.

[235] B. Toh, et al., Mesenchymal transition and dissemination of cancer cells is driven by myeloid-derived suppressor cells infiltrating the primary tumor, PLoS Biol. 9 (9) (2011).

[236] R. Lengagne, et al., T cells contribute to tumor progression by favoring pro-tumoral properties of intra-tumoral myeloid cells in a mouse model for spontaneous melanoma, PLoS One 6 (5) (2011), e20235.

[237] J. Eyles, et al., Tumor cells disseminate early, but immunosurveillance limits metastatic outgrowth, in a mouse model of melanoma, J. Clin. Invest. 120 (6) (2010) 2030–2039.

[238] A.V. Bazhin, et al., Cancer-retina antigens as potential paraneoplastic antigens in melanoma-associated retinopathy, Int. J. Cancer 124 (1) (2009) 140–149.

[239] M. Tham, et al., Macrophage depletion reduces postsurgical tumor recurrence and metastatic growth in a spontaneous murine model of melanoma, Oncotarget 6 (26) (2015) 22857–22868.

[240] F. Jain, et al., Endothelin signaling promotes melanoma tumorigenesis driven by constitutively active GNAQ, Pigm Cell Melanoma Res 33 (6) (2020) 834–849.

[241] O. Urtatiz, et al., GNAQQ209L expression initiated in multipotent neural crest cells drives aggressive melanoma of the central nervous system, Pigm Cell Melanoma Res 33 (1) (2020) 96–111.

[242] J.L.Y. Huang, O. Urtatiz, C.D. Van Raamsdonk, Oncogenic G protein GNAQ induces uveal melanoma and intravasation in mice, Cancer Res. 75 (16) (2015) 3384–3397.

[243] A.R. Moore, et al., GNA11 Q209L mouse model reveals RasGRP3 as an essential signaling node in uveal melanoma, Cell Rep. 22 (9) (2018) 2455–2468.

[244] C.P. Choe, et al., Transgenic fluorescent zebrafish lines that have revolutionized biomedical research, Lab Anim Res 37 (1) (2021) 26.

[245] M. Schartl, et al., A mutated EGFR is sufficient to induce malignant melanoma with genetic background-dependent histopathologies, J. Invest. 130 (1) (2010) 249–258.

[246] B. Ju, et al., Co-activation of hedgehog and AKT pathways promote tumorigenesis in zebrafish, Mol. Cancer 8 (2009).

[247] M.A. Mouti, et al., Minimal contribution of ERK1/2-MAPK signalling towards the maintenance of oncogenic GNAQQ209P-driven uveal melanomas in zebrafish, Oncotarget 7 (26) (2016) 39654–39670.

[248] D.E. Perez, et al., Uveal melanoma driver mutations in GNAQ/11 yield numerous changes in melanocyte biology, Pigm Cell Melanoma Res 31 (5) (2018) 604–613.

[249] G.B. Phelps, et al., MITF deficiency accelerates GNAQ-driven uveal melanoma, Proc. Natl. Acad. Sci. U. S. A. 119 (19) (2022).

[250] A.C. Thomas, et al., Mosaic activating mutations in GNA11 and GNAQ are associated with Phakomatosis Pigmentovascularis and extensive dermal Melanocytosis, J. Invest. Dermatol. 136 (4) (2016) 770–778.

[251] G.B. Phelps, et al., MITF deficiency and oncogenic GNAQ each promote proliferation programs in zebrafish melanocyte lineage cells, Pigm Cell Melanoma Res 35 (5) (2022) 539–547.

[252] R. Baghban, et al., Tumor microenvironment complexity and therapeutic implications at a glance, Cell Commun. Signal. 18 (1) (2020) 59.

[253] J. Madic, et al., Pyrophosphorolysis-activated polymerization detects circulating tumor DNA in metastatic uveal melanoma, Clin. Cancer Res. 18 (14) (2012) 3934–3941.

[254] F. Roula, et al., BAP1 deficient human and mouse uveal melanomas up-regulate a shared EMT pathway, bioRxiv (2023) (p. 2023.05.24.542173).